

REPORT DOCUMENTATION PAGE

Form Approved OMB No. 0704-0188

Public reporting burden for this collection of information is estimated to average 1 hour per response, including the time for reviewing instructions, searching existing data sources, gathering and maintaining the data needed, and completing and reviewing the collection of information. Send comments regarding this burden estimate or any other aspect of this collection of information, including suggestions for reducing the burden, to Department of Defense, Washington Headquarters Services, Directorate for Information Operations and Reports (0704-0188), 1215 Jefferson Davis Highway, Suite 1204, Arlington, VA 22202-4302. Respondents should be aware that notwithstanding any other provision of law, no person shall be subject to any penalty for failing to comply with a collection of information if it does not display a currently valid OMB control number.

PLEASE DO NOT RETURN YOUR FORM TO THE ABOVE ADDRESS.

1. REPORT DATE (DD-MM-YYYY) 29-12-2008	2. REPORT TYPE Final Report	3. DATES COVERED (From – To) 01-May-06 - 14-May-10
--	---------------------------------------	--

4. TITLE AND SUBTITLE Control of Heat Fluxes on the Surface of the Body Streamlined by Supersonic Flow with the Help of MHD Method	5a. CONTRACT NUMBER ISTC Registration No: 3475
	5b. GRANT NUMBER
	5c. PROGRAM ELEMENT NUMBER

6. AUTHOR(S) Dr. Sergey Vasilievich Bobashev	5d. PROJECT NUMBER
	5d. TASK NUMBER
	5e. WORK UNIT NUMBER

7. PERFORMING ORGANIZATION NAME(S) AND ADDRESS(ES) Ioffe Physico-Technical Institute of Russian Academy of Sciences 26, Polytekhnicheskaya St. Petersburg 194021 Russia	8. PERFORMING ORGANIZATION REPORT NUMBER N/A
--	--

9. SPONSORING/MONITORING AGENCY NAME(S) AND ADDRESS(ES) EOARD Unit 4515 BOX 14 APO AE 09421	10. SPONSOR/MONITOR'S ACRONYM(S)
	11. SPONSOR/MONITOR'S REPORT NUMBER(S) ISTC 05-7004

12. DISTRIBUTION/AVAILABILITY STATEMENT

Approved for public release; distribution is unlimited.

13. SUPPLEMENTARY NOTES

14. ABSTRACT

This report results from a contract tasking Ioffe Physico-Technical Institute of Russian Academy of Sciences as follows: The contractor shall numerically and experimentally investigate the processes accompanying pulsed magnetic impacts on a high-velocity flow of ionized gas, in particular, its effect on drag and heat flux. The project is divided into the following 8 well defined tasks: Task1: Design and fabricate the model a flat plate with embedded electrodes. Adapt the algorithm and codes for the numerical simulation of an essentially non-stationary hypersonic flow of a viscous heat conducting plasma exposed to a pulsed magnetic field. Develop an acceptable design of the gradient heat flux sensor. Task 2. Choose the experimental flow regime and plasma parameters. Calculate the flow parameters in the test channel in a regime of an MHD generator. Task 3. Carry out measurements and calculations aimed at revealing the influence of a magnetic field on the heat flux toward the flat plate. Task 4. Analyze the experimental results, comparison with the results of calculations and make conclusions concerning an electrodeless scheme of the MHD interaction around a body of revolution. Task 5. Design and manufacture the model a body of revolution with an induction coil housed inside. Update the design of the gradient heat flux sensor: evaluation of the necessary sensitivity and placement. Task 6.- Mount the heat flux sensors and document the measurement system performance. Task 7. Search the test space of flow parameters and magnetic field strength that induce an electric current around the test object. Conduct numerical simulations of the MHD plasma flow about the test object. Task 8. Carry out measurements aimed at revealing the influence of a magnetic field on the heat flux toward the surface of a body of revolution. Analysis of the results.

15. SUBJECT TERMS
EOARD, Physics, Plasma Physics and Magnetohydrodynamics

16. SECURITY CLASSIFICATION OF:			17. LIMITATION OF ABSTRACT UL	18. NUMBER OF PAGES 44	19a. NAME OF RESPONSIBLE PERSON SURYA SURAMPUDI
a. REPORT UNCLAS	b. ABSTRACT UNCLAS	c. THIS PAGE UNCLAS			19b. TELEPHONE NUMBER (Include area code) +44 (0)1895 616021

ISTC Project No. 3475p

**Control of heat fluxes on the surface of the body
streamlined by supersonic flow
with the help of MHD method**

Final Project Technical Report

on the work performed from May 1, 2006 to October 31, 2008

Ioffe Physico-Technical Institute

Project Manager

Prof., Dr., S.V. Bobashev

Director

Prof., Dr., V.A. Dergachev

October 2008

This work is supported financially by EOARD and performed under the contract to the International Science and Technology Center (ISTC), Moscow.

Title of the Project: Control of heat fluxes on the surface of the body streamlined by supersonic flow with the help of MHD method

Commencement Date: May 1, 2006

Duration: 10 quarters

Project Manager Prof., Dr., S.V. Bobashev

phone number: +7-812-2929153

fax number: +7-812-2971017

e-mail address: s.bobashev@mail.ioffe.ru

Leading Institute: Ioffe Physico-Technical Institute
Politekhicheskaya, 26
(812) 297-22-45
www.ioffe.ru

Keywords:

Abstract	5
Review of the basic experimental results obtained in the course of fulfillment of the Project	6
Implementation of the MHD impact on the supersonic flow of a molecular gas about a body of revolution	6
Results of the optical measurements	8
Results of thermal measurements.....	9
Development of the technique of measurements of heat fluxes with the help of gradient sensors on the surface of an object.....	11
References	13
NUMERICAL SIMULATION	25
ABSTRACT	25
COMPRESSION FLOW IN THE DIHEDRAL ANGLE	25
Mathematical model.....	25
Boundary conditions	26
Numerical method.....	26
Some results.....	27
Conclusions	31
SUPERSONIC FLOW AROUND CONE-CYLINDER MODEL BODY	31
Mathematical model.....	32
Numerical method.....	32
Some results.....	32
Conclusion.....	36
Attachment 1: List of published papers and reports with abstracts.....	37
Attachment 2: List of presentations at conferences and meetings with abstracts	41

NOMENCLATURE

l_D	–	Debye length
L	–	characteristic length
V_0	–	characteristic velocity
c	–	speed of light
ω_p	–	plasma frequency
Re_m	–	magnetic Reynolds number
ρ	–	plasma density
\vec{V}	–	plasma velocity
T	–	plasma temperature
μ	–	plasma viscosity
λ	–	plasma thermal conductivity
\vec{B}	–	induction of magnetic field
\vec{E}	–	electric field strength
\vec{j}	–	electric current density
ε	–	specific internal plasma energy
\vec{P}	–	stress tensor
\vec{S}	–	velocity strain tensor
E	–	total plasma energy
μ_e	–	effective viscosity
λ_e	–	effective thermal conductivity
Pr	–	Prandtl number
Pr _t	–	turbulent Prandtl number
σ	–	plasma electric conductivity
k	–	loading coefficient
ν	–	modified turbulent viscosity
G_ν	–	turbulence generation
Y_ν	–	turbulence dissipation

Abstract

The first section of the final report on the works according to ISTC Project (2006–2008 including the extension of the Project for 9th and 10th stages) contains the review of the basic experimental results of MHD influence on a supersonic gas flow, results of numerical simulation of the processes in a supersonic viscous flow as well as the analysis of them.

The second section of the report is devoted to development of a technique for employment of the gradient heat flux sensor (GHFS) which at present is the only accessible instrument being capable of functioning in the presence of strong electromagnetic interference.

The investigation is carried out of the MHD influence on the flow about two models in the shape of a cone mated with a cylinder. At the cone vertex and along the mating line two electrodes are located between that an electric discharge is implemented, and inside the cylindrical parts a magnetic inductor is housed. One of the models is equipped with a magnetic core inside the inductor. An appreciable difference between the influences on the gas flow about these two models was detected.

Dependence of the MHD influence on the flow about the models depending on the polarity of connection of the electrodes to an external voltage source is found.

Because of the large thickness of the GHFS its signal is proportional to the temperature but not to the heat flux, a procedure of transformation of the GHFS signal into the heat flux is developed. Evaluations of the errors of the temperature measurements and determination of the heat flux are carried out.

The comparison is drawn between the results obtained with the help of the GHFS and the data of direct measurements by the Atomic Layer Thermo Pile. The conclusion is drawn on the applicability of the GHFS and technique of processing of its signal in investigations of pulsed magnetohydrodynamic processes of a moderate duration (~ 1 ms).

Review of the basic experimental results obtained in the course of fulfillment of the Project

According to the Project topic the authors had two problems before them: to investigate capabilities of a magnetohydrodynamic (MHD) influence on the supersonic flow about a body and to develop a technique for determination of the heat flux toward the object surface caused by a pulsed heat load.

In investigations [1–3] carried out earlier it was shown that the MHD impact implemented in a bounded region of a supersonic flow (local MHD interaction) was capable of effective influence on the downstream gasdynamic parameters including the heat flux toward the body surface. In those experiments, the magnetic field was established over the whole volume of the test section, and the local character of the MHD interaction was conditioned by passing an electric current in a bounded region of the supersonic flow. The magnetic field and direction of the current flowing through the flow were oriented so that the ponderomotive force was parallel to the flow velocity vector. Reversing the direction of the electric current flowing through the gas flow changed the direction of the ponderomotive force.

Analysis of the results obtained and the capabilities of the experimental setup enabled us to design a model (in the shape of a cone mated with a cylinder) bearing all elements that are necessary for implementation of an MHD impact. The pulsed magnetic field is induced by a discharge of an external voltage source through the inductor located under the cylindrical model surface. The central electrode shapes the cone vertex, and on the conical model part near the line of mating the cone with cylinder the second ring electrode is located. The gas discharge between the electrodes in the presence of the magnetic field of the inductor starts to rotate under the action of the ponderomotive force directed, in this case, normally to the velocity vector of the mainstream. The influence on the flow is conditioned by two main factors: by the heat release due to the passage of the electric current and by the action of the ponderomotive force. Studying the MHD influence on the supersonic flow with the use of the configuration described has become one of the investigation subjects in the present Project.

The thermal measurements were carried out by the gradient heat flux sensor (GHFS) fabricated on the base of anisotropic Bismuth monocrystal [4]. The GHFS is characterized by a short time of response, high sensitivity and noise immunity due to its structure. At present these sensor properties do not leave an alternative in the choice of means for thermal measurements in pulsed processes in the presence of strong electromagnetic fields.

However direct measurements of the heat flux in pulsed processes with the duration of some milliseconds with the help of the GHFS is impossible because of the thermal lag of this sensor. For determination of the heat flux the sensor signal is subjected to the mathematical processing by the technique developed. Elucidation of the domain of applicability of this technique as well as uncertainty of determination of the heat flux using the measurement data constitute the second part of the investigations in the present Project.

Implementation of the MHD impact on the supersonic flow of a molecular gas about a body of revolution

In the course of fulfillment of the Project we tested two models in the shape of a body of revolution consisting of a 60° cone mated with a cylinder of 28 mm in diameter. Under the cylindrical surface of the models (Figs. 1 and 2) magnetic inductor (2) is located. The inductor consists of 17 turns of a copper wire of 1 mm in diameter. One of the models contains iron core (1) located coaxially with the model (5). The core is fabricated from soft steel (ARMCO) with low residual magnetization. The core serves as a magnetic circuit and amplifier of the magnetic field [5]. The operation of the electromagnetic facility of the model with the core was provided by one external voltage source consisting of a set of inductive (L) and capacitive (C) elements.

One of terminals of the voltage source was connected with central electrode (4) and the other was connected with one of the ends of inductor (2). The other end of the inductor was connected with ring electrode (3) so that the emergence of the gas discharge (6) between electrodes (3) and (4) closed the discharge circuit of the voltage source. In this case, the currents flowing in discharge (6) and inductor (1) are the same.

The model without core (Fig. 2) was capable of operating with one source, like the previous model, as well as a regime of operation with two independent sources could be implemented: for the magnetic system (source E_1) and for the gas discharge (source E_2). This enabled us to implement independent variations of the currents flowing through the discharge gap and inductor. In this case, the current flowing through the magnetic system was triggered by vacuum arrester (VD) at the moment of onset of gas discharge (6).

The heat sensor was located at the center of the generatrix of the cylindrical model surface (see Figs. 1 and 2).

The experiments were carried out at the Ioffe Institute Big shock tube with the use of the available test section containing the supersonic nozzle. The model under study was located in the output nozzle cross section (Fig. 4). The parameters of the supersonic nitrogen flow at the nozzle output were: pressure – 4.3 kPa, temperature – 600 K, density – 0,025 kg/m³, flow velocity ~2 km/s, Mach number – 4, duration of stationary flow ~1.5 ms.

Actuation of the electromagnetic facility was implemented either by a triggering high-voltage pulse with a duration of ~ 1 μ s which was applied into the circuit of the gas discharge, or spontaneously due to formation of the flow in the nozzle. In the latter case, the voltage of the source, i.e. the initial voltage between the electrodes amounted to not less than 500 V. The duration of the gas discharge pulse amounted to ~ 2 ms and the amplitude reached 2 kA, the duration of the current pulse in the inductor (at the independent power supplies) amounted ~ 1 ms (see Fig. 3) and the amplitude varied up to 8 kA.

In the experiments we recorded Schlieren patterns of the flow about the models, the total discharge glow from the vicinity of the model recorded during the whole process, optical scanning of the discharge glow against the bounded area of the conical surface, as well as pulses of the currents flowing through the inductor and gas discharge.

Distributions of the magnetic induction along the cone generatrix of the models under study appreciably differ from one another due to the presence of the magnetic core inside one of them. For measurements of the magnetic induction we used a test magnetic coil of 5 mm in diameter. The coil was located on the conical surfaces of the models at two points: near the ring electrode and in the middle of the discharge gap. The coil axis was oriented normally the cone surface.

Before the measurements, the inductors of both models were connected in series into the circuit of the pulsed voltage source. In the course of the discharge the test coil signal was recorded. Integrating this signal with respect to time enabled us to determine variation of the magnetic induction at the points of measurements. Figure 5 shows variations of the magnetic induction at the two above-mentioned points of the discharge gap near the conical surface for both models. Magnitude R in the plot corresponds to the radius of the cone cross section passing through the measurement point. In the plot is seen that the magnetic induction near the model containing the core is higher. In this case, the maximum of the magnetic induction is attained noticeably later than for the model with no core.

Figure 6. shows a supposed distribution of the of the magnetic induction along the cone generatrix at the moment ~ 0.6 ms from the discharge onset. Signs in the plot mark the measurement results, lines – the supposed distributions. In the cross section of the end of the magnetic core at

$x = 7$ a drastic variation of the magnetic induction occurs.

Below in the text we shall use the maximum of the magnetic induction B_m on the cone surface near the ring electrode as the scale of the magnetic induction.

Results of the optical measurements

The most dramatic difference detected when comparing patterns of the flow about the models under study is related with the gas discharge structure and the extent of its influence on the flow about the models. Figure 7 shows Schlieren patterns of the supersonic nitrogen flow with Mach number 4 about the models. In Fig. 7, a there is a typical pattern of the stationary flow with no MHD influence, Figs. 7, b, c show the flows about the models with the magnetic core and without it, respectively.

Comparison between the first pattern and the subsequent ones allows us to affirm that the electric discharge rotates around the model disturbing not only the flow downstream but also affects the bow shock wave in the vicinity of the model nose where the central electrode is located. Patterns in Figs. 7, b, c correspond to the experiments carried out at the same gasdynamic flow parameters and discharge currents. In this case, the power supply of the model with no magnetic core was the same as for the model containing the magnetic core, and the currents flowing through the inductors were the same. The maximum magnitudes of the current and magnetic induction amounted to $I_m = 1.7 \text{ kA}$ и $B_m = 0.3 \text{ T}$ for the model with no core, and $I_m = 1.5 \text{ kA}$ и $B_m = 0.7 \text{ T}$ for the model with the core, respectively. In spite of that the electric energies deposited into the gas discharges are approximately the same for both models, the strong difference between the discharge glows in Figs. 7, b, c attracts one's attention. In addition, in Fig. 7, b where the luminosity is higher, there are strong perturbations of the flow about the cylindrical model surface, and in Figs. 7, c, they are invisible.

For evaluation of the velocity of the plasma rotation around the body we used a waiting photo recorder. The object image focused onto a film moved over the film with the help of a rotating mirror prism at a preset speed. The image size in the direction of optical scanning was bounded with the help of a slit diaphragm. The slit of the recorder of 2 mm in width was oriented parallel to the cone generatrix and the image included the cone vertex and base.

Figure 8 shows a fragment of the optical scanning of the discharge glow against a bounded area of the conical part of the model with the magnetic core. The horizontal direction corresponds to the time axis, and the upward direction corresponds to moving from the cone vertex to the cone base. In Fig. 7 one can see that the discharge occupies a bounded area and at a certain instant the plasma rotation acquires a periodic character.

When observing the discharge near the model with no magnetic core we failed in detecting variation of the discharge luminosity, probably, due to its weakness. Variations of the luminosity when increasing the magnetic induction up to $B_m = 0.7 \text{ T}$ were also not detected.

Analysis of the data of optical scanning and Schlieren patterns enables us to affirm that the gas discharge near the model containing the magnetic core is localized in a comparatively narrow flow region. The discharge near the model with no core, apparently, is distributed more uniformly (spreads) over the cone surface. Since the electric energies depositing into the discharges near both models are the same, the density of the electric current near the model containing the core turns out to be higher than near the model with no core. The same also concerns the plasma temperature in the discharge and, consequently, the luminosity of the plasma glow.

The reasons for such a difference between the sizes of the discharge regions, probably, should be searched in the distribution of the magnetic induction along the discharge gap. Elucidate what we have in mind by a simple example. In order that a linear discharge when rotating around a conical surface would remain parallel to the cone generatrix, the ponderomotive force must vary along the discharge length in such a way that the angular rotation velocity at all points of the discharge would remain constant. The rotational motion of the volume unit of the discharge in our case is governed by the ponderomotive force:

$$\rho \cdot \omega^2 r = jB(r),$$

where ω is the angular velocity, r is the radius, ρ is the plasma density, j is the density of the discharge current, B is the magnetic induction. Assuming that the current remains constant along the discharge length we write the condition of independence of the angular velocity on radius in the form $\frac{B(r)}{r} = const.$

Proceeding from the estimates proposed let us peek at the distributions of $B(r)/r$ along the cone generatrix that took place in the experiments with the two models. Figure 9 shows variations of ratio B/r at two points of the discharge gap for the two models. In the plot is seen that two curves corresponding to the model containing the magnetic core and describing variation of the magnetic induction in two cross sections practically coincide during a time interval of ~ 0.4 ms from the process beginning. This means that during this time interval the gas discharge channel deformation by the magnetic field is minimal. For the model with no magnetic core coincidence of the two corresponding curves are not observed during the whole process, which, apparently, leads to spreading of the discharge over the cone surface at velocities varying with distance from the cone vertex.

Another distinctive of the object under study is the dependence of the gas discharge dynamics on the polarity of connection of the electrodes to the voltage source energizing the discharge. This distinctive manifests itself identically when testing both models under study and consists in that at other conditions being equal the discharge rotation frequency is higher when the ring electrode is the cathode, i.e. when it is connected to the negative terminal of the voltage source. Detecting the rotation frequency of the discharge around the model with the magnetic core was conducted on the base of the optical scanning. In this case, the discharge rotation frequency amounted to ~ 30 kHz when the ring electrode was cathode, and ~ 15 kHz at the positive polarity of the ring electrode. The electric parameters were: discharge current $I_m = 1.5$ kA and magnetic induction $B_m = 0.7$ T.

When testing the model with no core, the influence of reversing the polarity of the electrodes was studied in other way (in this case, the optical scanning was ineffective because of low brightness of the discharge). We recorded on a film the discharge glow during whole experiment at a comparatively weak discharge current. Figure 10 shows photographs corresponding to the opposite polarities of the ring electrode. The photographs was taken in a regime of operation of the electromagnetic facility energized by one voltage source when the maximum discharge current amounted to $I_{max} = 1.5$ kA, and magnetic induction was $B_m = 0.3$ T. In Fig. 10 is seen that when the ring electrode is anode (positive polarity) the discharge glow near the model is asymmetric, which points out that the plasma during the experiment has no time to execute the whole turn around the model. At the reverse polarity of the ring electrode the discharge executed, at least, one whole turn and the light-striking looks more symmetrically.

Results of thermal measurements

Keeping in mind the results of optical observations described above let us turn to analysis of the thermal measurements. Since the actual magnitude of the heat flux in the physical processes under study is not determinative, as the illustrative material we shall demonstrate the electrical signals of the heat flux sensors.

Figure 11 shows signals of the heat sensor located on the cylindrical surface of the model containing the magnetic core. In the plot there are signals at various discharge currents and magnetic inductions ($I_m = 1.3$ kA, $B_m = 0.6$ T and $I_m = 1.5$ kA, $B_m = 0.7$ T) obtained at the positive and negative polarities of the ring electrode.

Analyzing magnitudes of the signals we should note a very remarkable fact. When increasing the discharge current and magnetic induction the magnitude of the signal of the heat sensor varies differently: when the ring electrode is positive the mean magnitude of the signal

increases, and at the negative polarity of the ring electrode the signal decreases. This fact demonstrates in principle a capability of controlling the heat flux toward the surface of an aircraft with the help of the MHD approach.

When considering in more detail one can find in the signal spectrum periodic pulsations whose frequency increases and their amplitude decreases with increasing the current.

Dependence of the pulsation frequency on the polarity of the ring electrode is found: when the polarity is negative the pulsation frequency is higher, when the polarity is positive the frequency is lower. It should be noted that magnitudes of the rotation frequency recorded by the heat sensor well correspond to the discharge rotation frequency measured with the use of optical scanning.

The thermal measurements on the surface of the model with no magnetic core were carried out both in the regime of operation with the single voltage source (like with the model containing the core) and at independent power supplies of the inductor and discharge. In this case, such vivid distinctions that were observed in experiments with the model containing the core were not found. In the spectrum of signals of the heat sensor there are no pulsations that took place when testing the model with the core. Besides, from test to test there was no reproducibility of the shape of the heat sensor signal at the same initial conditions of the experiments. Figure 12 shows sensor signals (solid lines) corresponding to experiments with the following parameters of the discharge and magnetic field $I_m = 1.5$ kA, $B_m = 0.3$ T. The dashed line in the plot indicates variation of the magnetic induction. It is seen that during the action of the magnetic field the signals considerably differ from one another. Probably, this is associated with that the duration of one turn of the discharge around the model is comparable with the process duration (see Fig. 10). For this reason the signal shape may largely depend on the mutual azimuthal positions of the sensor and the discharge at the moment of its initiation.

Some peculiarity in the behavior of the gas discharge was found in experiments with the model without core at magnitudes of the magnetic induction close to $B_m = 0.7$ T. In these experiments a strong influence of the magnetic field on the gas discharge dynamics was observed.

Figure 13 demonstrates pulses of the currents flowing through the discharge and inductor corresponding to such a regime. In the plot is seen that at the initial instant a small variation of the discharge current is observed. This variation is sufficient for initiation of the current through the inductor (curve *I*). The discharge current remains weak and only in 0.3 ms from the process beginning it starts to grow attaining its maximum $I_{max} = 1.3$ kA. This process influences also on the heat sensor signal (see Fig. 14). In Fig. 14 is seen that at the initial instant a small variation of the signal occurs and to instant ~ 0.5 ms increase of the heat sensor signal is observed.

Such a behavior of the gas discharge, is apparently related with that in this regime the electric circuits of the discharge and magnetic inductor are independent from one another and the magnetic field being established during some time (the pulse rise time of the magnetic induction amounts to ~ 0.2 ms) “suppresses” the gas discharge. In the regime of model operation with the single voltage source the discharge current and the current flowing through the inductor are the same and the “suppression” effect is not observed.

In the course of fulfillment of the Project “Control of Heat Fluxes on the Surface of the Body Streamlined by Supersonic Flow with the Help of MHD Method” the experimental investigations of the supersonic nitrogen flow with Mach number 4 about the two models equipped with the electromagnetic facilities have been carried out. Distribution of the magnetic induction along the discharge gap, in our opinion, governs the extent of spreading of the discharge when rotating it, which recoils on the current density in the discharge. Experiments with the models under study were carried out at the practically equal depositions of the electric energy into the gas discharge. Since the discharge near the model with the magnetic core is more compact, in this case, the current density in the discharge is higher. Consequently, the gas

temperature inside the discharge is higher too (more intensive glow), and the gasdynamic perturbations are stronger.

The MHD effects, in particular the discharge rotation frequency, near the model with the core manifest themselves more forcibly than near the model without core. The reason for this consists in the larger ponderomotive force, which is proportional to the density of the electric current and to the magnetic induction. Remind that in the case of the model with the core the latter two quantities are appreciably higher than without core. The ponderomotive force swirls the gas around the model.

Influence of polarity of the electrodes on the discharge dynamics can be also explained by changes in local magnitudes of the ponderomotive force along the discharge due to difference in the density of the electric current in the vicinities of the cathode and anode.

Analysis of the results of the thermal measurements should be conducted taking into account that the indications of the heat sensor are governed by two factors: by the heating of the gas by the electric discharge and by changes in the gas parameters near the model surface caused by the gas rotation. In particular, under the action of the ponderomotive force, a displacement of the gas from the model surface toward the bow shock wave is possible. Since the gas rotation is governed by the ponderomotive force, the reverse of the electrode polarity is capable of influencing the flow and, consequently the indications of the heat sensor in a different way.

Development of the technique of measurements of heat fluxes with the help of gradient sensors on the surface of an object

As it was mentioned above, in pulsed processes with duration of some milliseconds the direct measurement of the heat flux with the help of the gradient heat flux sensor (GHFS) is impossible because of its thermal lag. However in experiments with MHD effects accompanied with strong electromagnetic interference there is no alternative to the GHFS at present.

For determination of the heat flux, the sensor signal is subjected to the mathematical processing [6, 7] which is based on the usage of the solution of the one-dimensional heat transfer equation for a half-space with the thermophysical parameters of the sensor material (Bismuth, in this case). This solution enables one to find the relation between the heat flux toward a surface and the change in its temperature. The solution has the simple form, which is convenient in practical applications. However, the usage of this solution is correct during a certain time interval beginning from the process onset until the heat exchange at the opposite sensor surface is negligible. According to our estimates for the GHFS of 0.2 mm in thickness this interval amounts to ~1 ms, which is sufficient for investigations of pulsed gasdynamic processes in a shock tube.

One of the important aspects of experimental investigations is the accuracy of the results being obtained. From the specificity of the processes under study and capabilities of the GHFS it follows that the accuracy of determination of the heat flux depends on the accuracy of the measurements themselves and errors introduced by the technique applied for processing the sensor signal. By the error introduced by the processing algorithm we mean the change in the relative error of the calculated heat flux after the procedure of nonlinear transformation of the temperature measurements as compared with the relative error of the temperature measurements themselves.

With the aim to determine the errors of measurements and reconstruction of the heat flux we carried out special experiments [8]. A model was fabricated whose sizes corresponded to the sizes of the model containing the electromagnetic facility. The appearance of the model is shown in Fig. 15. On the conical and cylindrical surfaces of the model six heat sensors were

installed. The model was located in flows of various gases (nitrogen, argon) with the parameters close to the ones in the experiments with the MHD interaction.

The measurement results were processed by the code developed for this aim and enabling us to calculate the heat flux on the base of measurement data, and then to evaluate the errors of the temperature measurements and the results of calculation of the heat flux. It was ascertained that the relative error of calculation of the heat flux amounted to approximately 10 % when the relative error of the temperature measurements was 1 %. One of the variants of such a calculation is shown in Fig. 16. In the top plot a distribution of the temperature of the GHFS surface (heat sensor signal) is shown, in the bottom plot there is the result of processing of the sensor signal in terms of the heat flux.

Since determination of the heat flux from the GHFS signal is associated with the use of the recalculation algorithm, it is important to draw a comparison between the results obtained and the data of the direct measurement of the heat flux. The direct measurement of the heat flux was carried out by the ALTP sensor (Atomic Layer Thermo Pile). The actual ALTP sensor is a film of 0.5 μm in thickness, consisting of canted alternating layers of $\text{YBa}_2\text{Cu}_3\text{O}_{7-d}$ and CuO_2 deposited onto a substrate of SrTiO_3 . The unit has a cylindrical shape of 6 mm in diameter and 3 mm in height. The active sensor dimensions of an ALTP can vary from 0.2×1 mm to 3×3 mm, depending on required spatial resolution in the experiment.

The sensor ALTP does not possess the necessary noise immunity for operation in the presence of strong electromagnetic fields therefore the data for the comparison were obtained in the absence of MHD impact.

The experiments were carried out at the Institute of Theoretical and Applied Mechanics of Siberian Branch of RAS (Novosibirsk, Russia) in the pulsed hypersonic wind tunnel IT-302.

The sensors GHFS and ALTP were installed at a plate located in a supersonic flow at the zero angle of attack being 183 mm distant downstream from the sharp leading edge. The distance between the sensors in the lateral direction was 16 mm. The gas parameters in mainstream were: Mach number $M = 6$, temperature 160 K, pressure ~ 0.1 bar.

Figure 17 shows dependencies of the absolute magnitude of the heat flux on time measured by the ALTP (curve 1) and GHFS (curve 2). The heat flux pulse recorded by the GHFS possesses the appreciably smaller amplitude as compared with the pulse of the ALTP. Because of a large thermal lag of the GHFS in the spectrum of its signal high-frequency pulsations are not observed, while they are present in the ALTP signal.

Curves 1 and 2 practically coincide only in 20 ms after the process beginning, this time corresponds to establishment of the stationary temperature distribution inside the GHFS. This enables us to affirm that the GHFS can be employed as a sensor for direct measurement of the heat flux in the processes with the characteristic duration more than 20 ms.

Figure 18 shows the absolute magnitudes of the heat flux measured by the ALTP (curve 1) and the result of processing of the GHFS signal with the use of technique described above (curve 2). It is seen that the maxima of both curves coincide in time, and the difference between the signal amplitudes appreciably decreases. It is remarkable that in the spectrum of the processed GHFS signal high-frequency pulsation with the period ~ 0.1 ms emerged. They practically coincide in time with the pulsation in curve 1.

In Fig. 18 is seen that after the instant ~ 0.7 ms the difference between curves 1 and 2 is relatively large. Possible reasons for that may be several. One of them may be related with the limitedness of the proposed technique for processing of the GHFS signal, namely, with the neglect of the process of the heat exchange at the boundary sensor–substrate.

Another reason may consist in the unhappy choice of the experiment conditions – small difference between the gas temperature (~ 160 K) and the plate surface (the initial plate and sensor temperature is ~ 290 K). It is known that the heat flux magnitude is proportional to the difference between the gas and the object surface (in the case considered, this difference

amounts to ~130 K). In the course of the warm-up the surface temperature changes depending of thermophysical properties of the surface. For example, in the test considered the temperature of the GHFS surface (Bismuth) changed by 7 K, while the temperature of the substrate of the ALTP – by 4 K. In such a case, the equality between the heat fluxes toward different surfaces is impossible. To elucidate the reasons for the difference in the indications of the two sensors and to expand the range of applicability of comparatively “thick” sensors in gasdynamic experiments it is necessary to resume the investigations.

In conclusion we say that the proposed technique for transformation of the electric sensor signal into the heat flux enables one to employ the GHFS for determination of the heat flux in pulsed processes with a duration of ~1 ms under conditions when employment of other means is impeded or impossible.

References

1. Bobashev S.V., Mende N.P., Sakharov V.A., Van Wie D.M. Magnetic field control of a supersonic nitrogen flow. Tech. Phys. Lett., v.30, 8. 2004. pp. 635-637.
2. Bobashev,SV; Mende,NP; Sakharov,VA; Van Wie,DM. Control of a supersonic nitrogen flow by a magnetic field. AIAA Meeting Papers on Disc, Vol. 10, No. 1-4 , pp. 5227-5231
43rd Aerospace Sciences Meeting and Exhibit, 10 - 13 January 2005, Reno, Nevada
3. Technical report no. 1. ISTC Project 3475p. July 2006.
4. Patent Number: EP 1223411. Universal sensor for measuring shear stress, mass flow or velocity of a fluid or gas, for determining a number of drops, or detecting drip or leakage. Di vin N.P., Mitiakov A.V., Mitiakov V.Y., Sapozhnikov S.Z. Publication date: 2002-07-17.
5. Technical report no. 4. ISTC Project 3475p. April 2007.
6. Technical report no. 6. ISTC Project 3475p. October 2007.
7. Reznikov B.I., Mende N.P., Popov P.A., Sakharov V.A., Shteinberg A.S. Determining heat flux from surface temperature measurements in pulsed gasdynamic processes. Tech. Phys. Lett., v.34, 8. 2008, pp. 656-658.
8. Technical report no. 3. ISTC Project 3475p. January 2007.

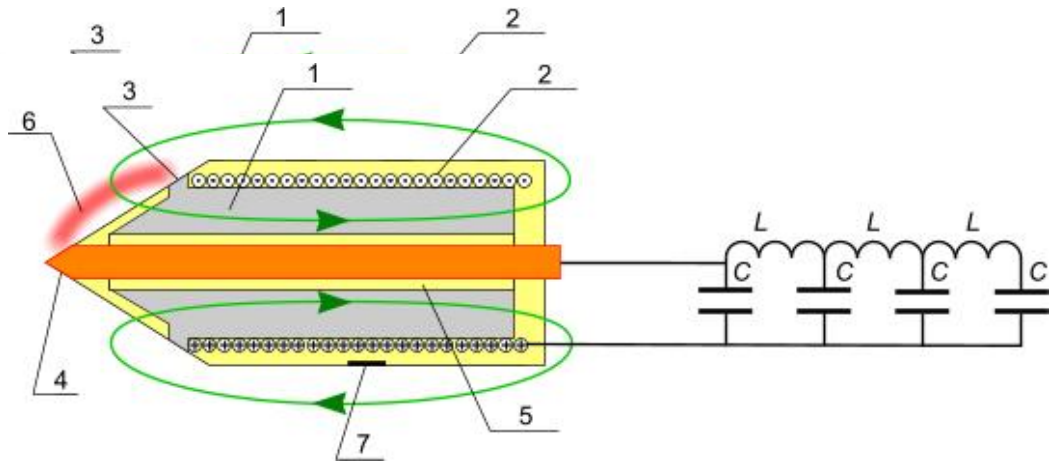


Fig. 1. Schematic of a model equipped with the electromagnetic facility.
 1 – magnetic inductor; 2 – core; 3 – ring electrode; 4 – central electrode;
 5 – insulator; 6 – gas-discharge plasma; 7 – heat sensor.

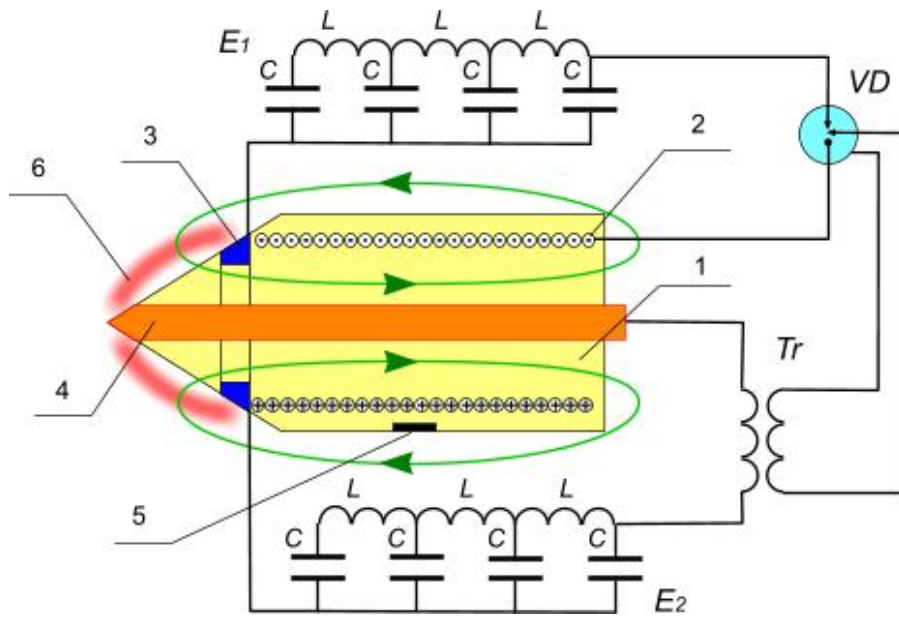


Fig. 2. Schematic of the model without magnetic core.

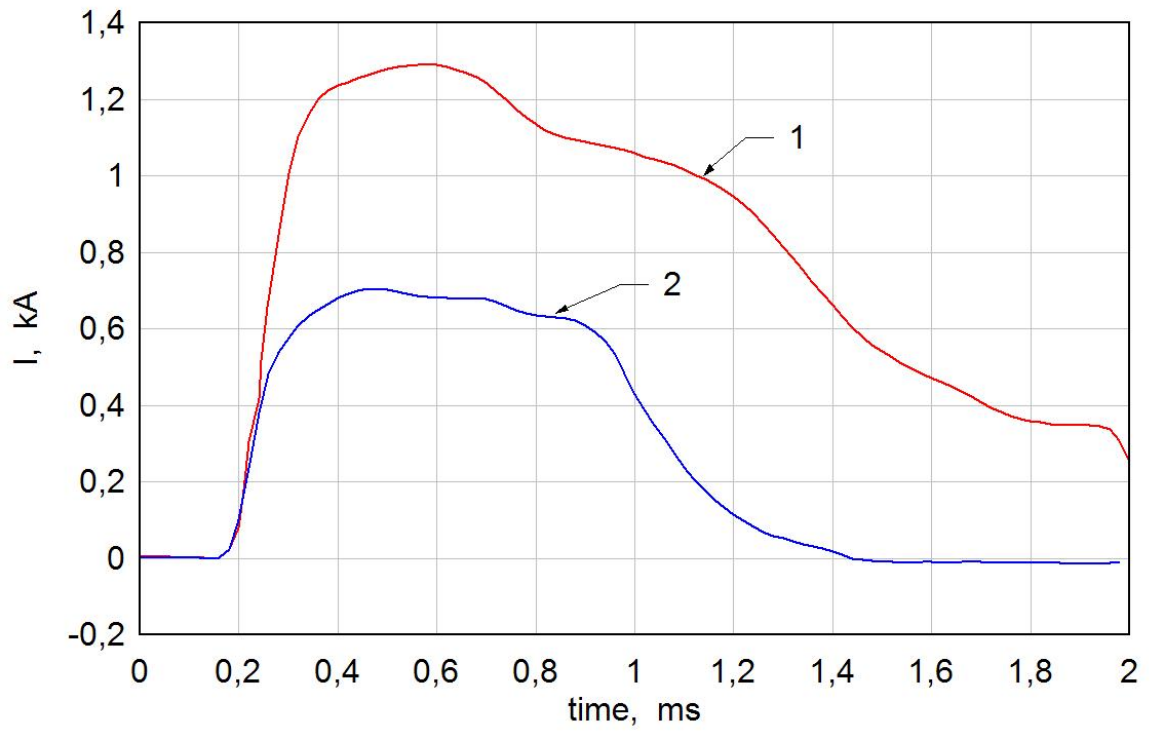


Fig. 3. Pulses of the currents flowing through gas discharge (1) and magnetic inductor.

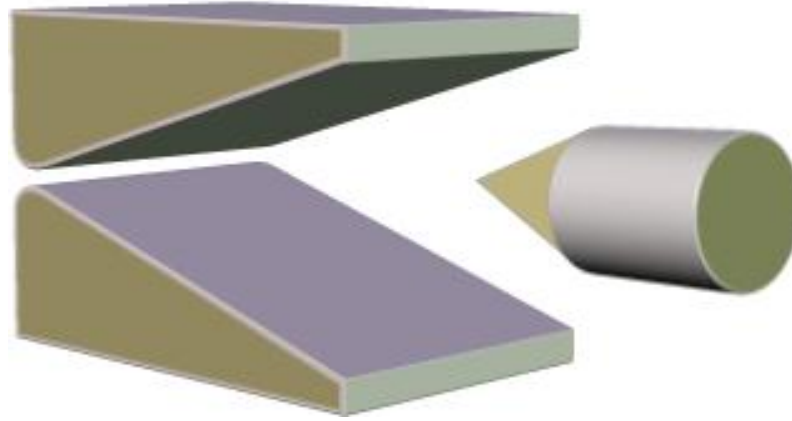


Fig. 4. Wedge-shaped supersonic nozzle and model.

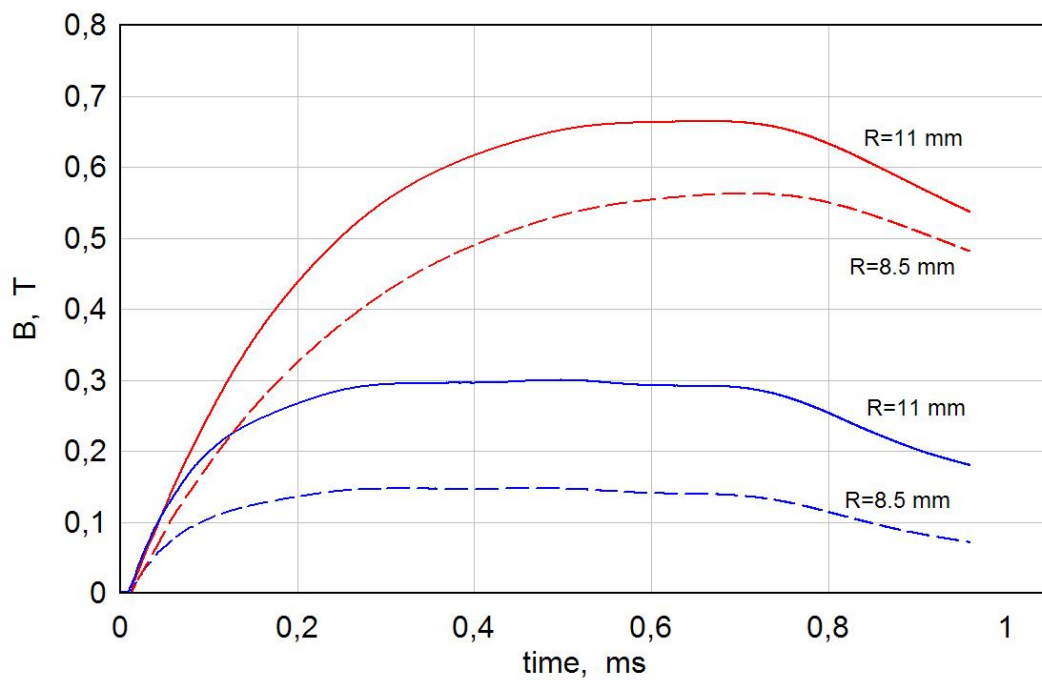


Fig. 5. Variation of the magnetic induction near the ring electrode ($R=11$ mm) and at the middle of the discharge gap ($R=8.5$ mm) for the model containing the magnetic core (top curves) and for the model without core (bottom curves).

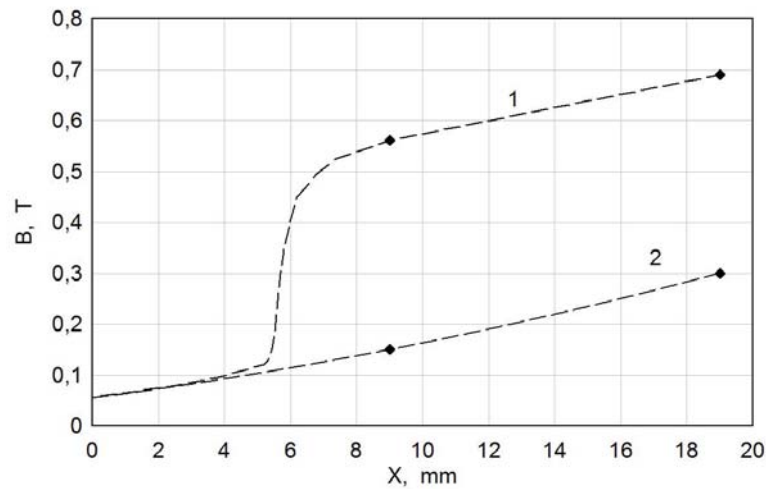


Fig. 6. The supposed distributions of the maximum magnetic induction (dashed lines) for the model with the magnetic core (1) and without core (2), along the generatrix of the conical model surface in the direction from the central electrode ($x=0$) to the ring one ($x=19$). The dots indicate the results obtained with the help of the test magnetic coil.

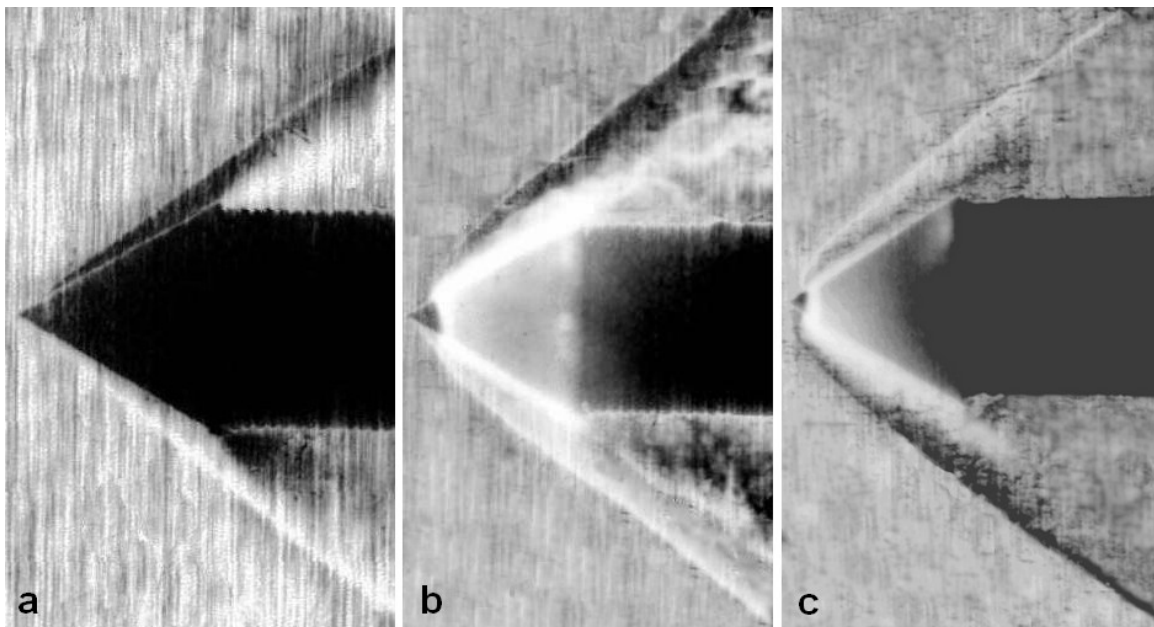


Fig. 7. Schlieren patterns of the supersonic nitrogen flow with Mach number 4:

- a) – without MHD interaction;
- b) – model containing magnetic core;
- c) – model without magnetic core.



Fig. 8. Optical scanning of the discharge glow against a bounded area of the conical surface of the model containing the magnetic core.

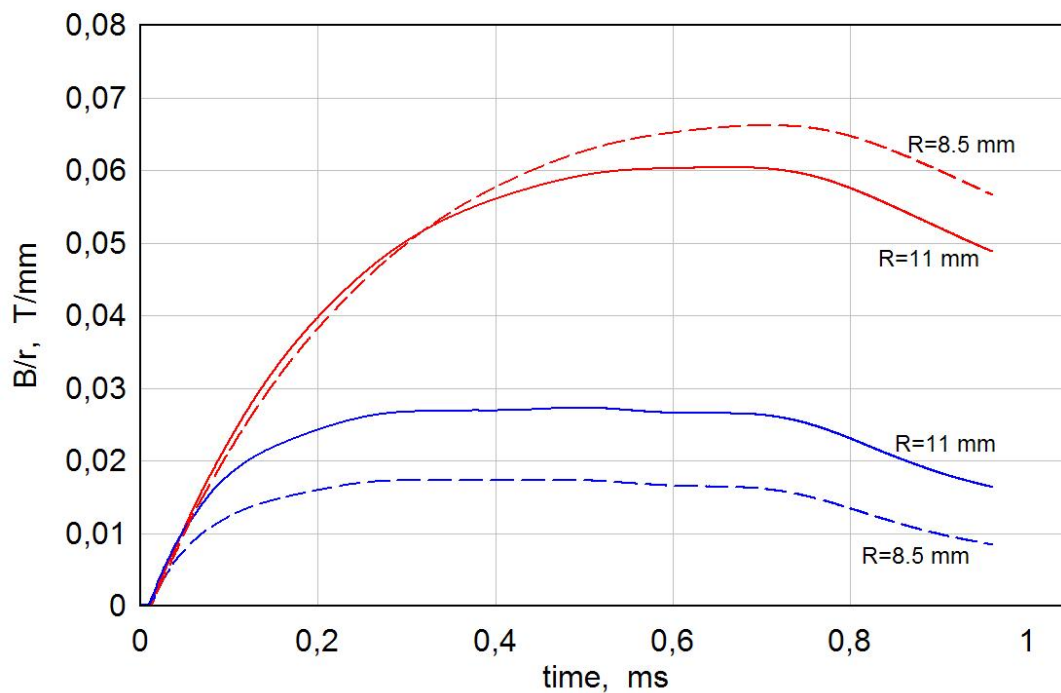


Fig. 9. Variation with time of the ratio of the magnetic induction to the radial coordinate of the points of measurements B/r for the model with the magnetic core (top curves) and for model without core (bottom lines).

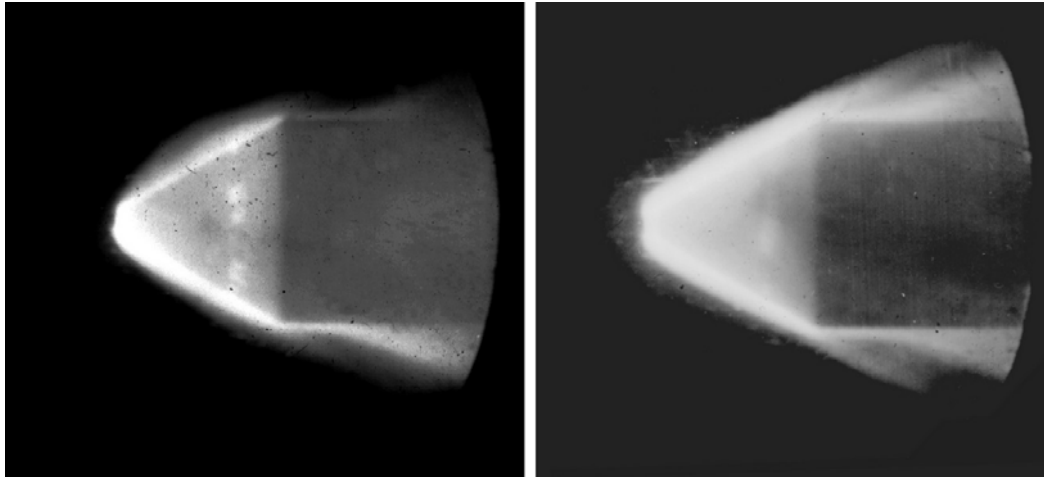


Fig. 10. Glow of the rotating discharge at the positive polarity (left) and negative polarity (right) of the ring electrode.

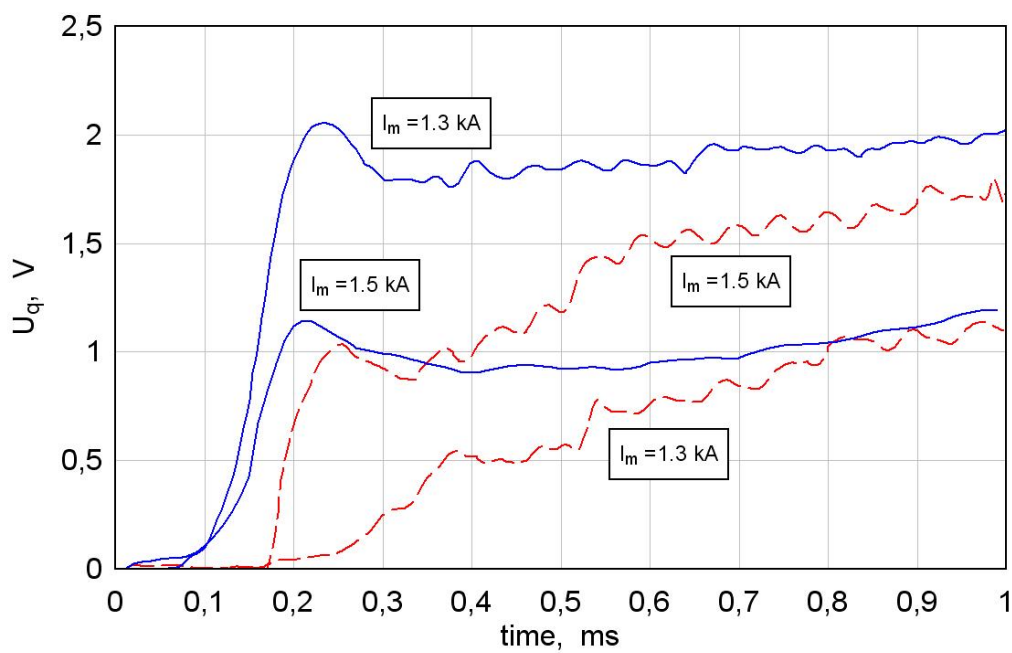


Fig. 11. Oscillograms of the signals of the heat flux sensors installed at the model with the core at the positive polarity (dashed lines) and negative polarity (solid lines) of the ring electrode.

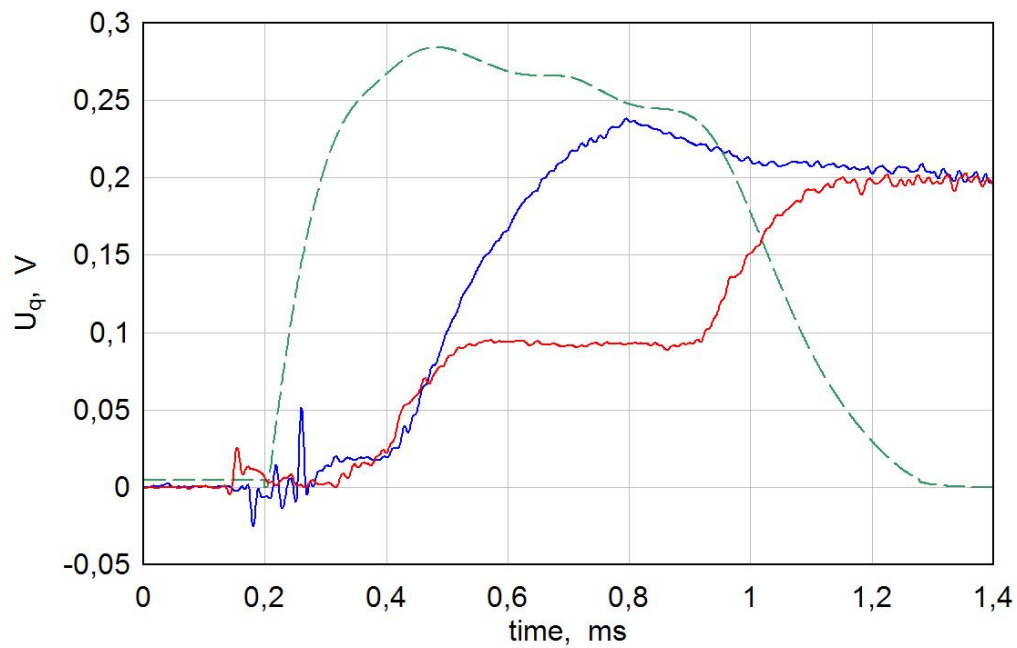


Fig. 12. Signals of the heat flux sensor (solid lines) and the pulse of the magnetic induction (dashed line) at the independent power supplies of the magnetic system and the discharge at the model without magnetic core.

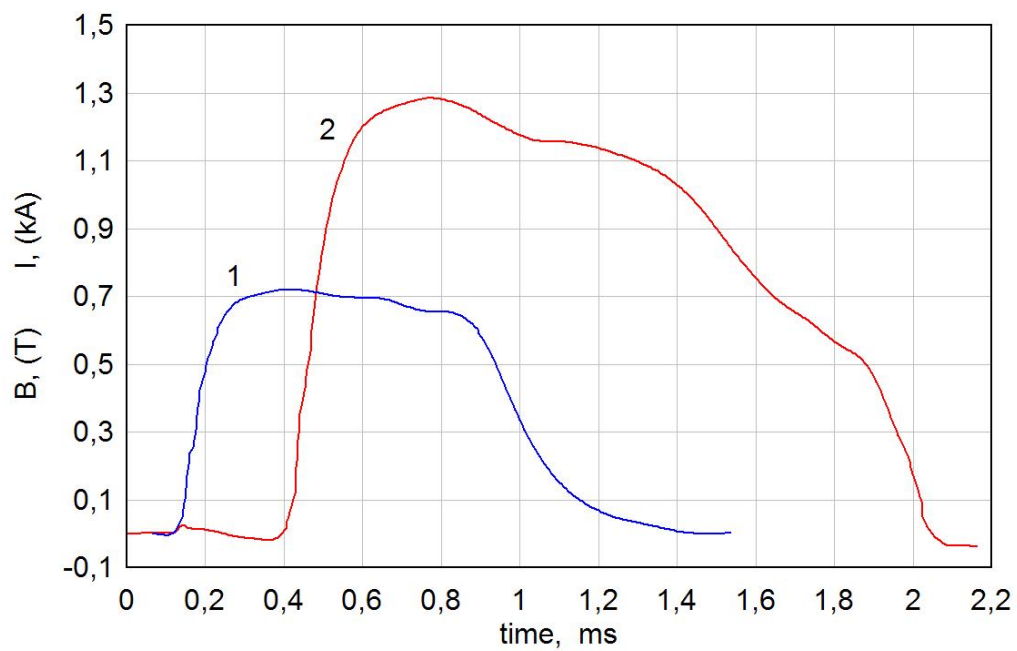


Fig.13. Influence of the magnetic induction (curve 1) on the discharge current (curve 2).

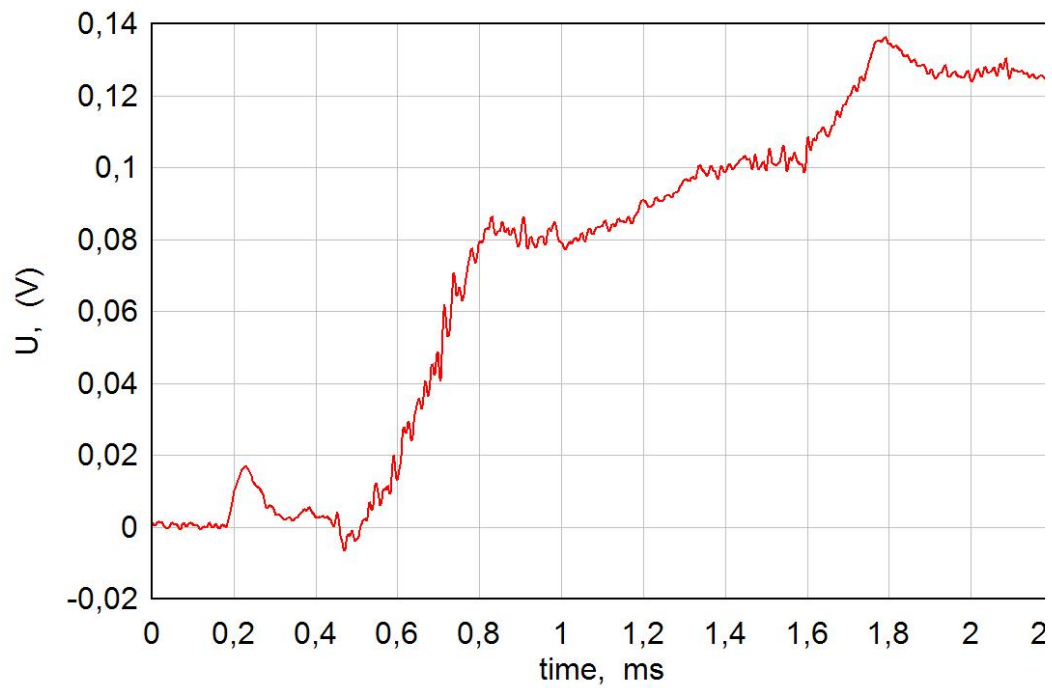


Fig. 14. Signal of the heat flux sensor when the magnetic field influences the discharge.



Fig. 15. Appearance of the model with six heat sensors on the surface.

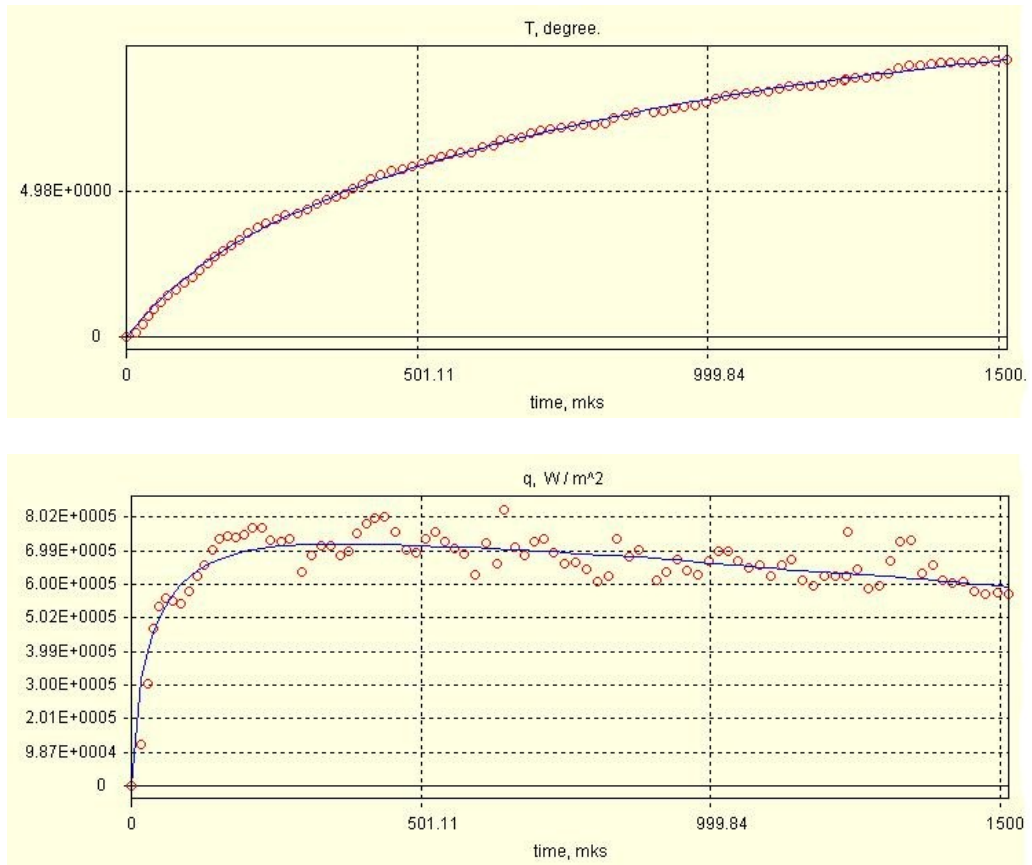


Fig. 16. Variation with time of the sensor surface temperature (top plot) and the calculated heat flux (bottom plot). Signs indicate the data of measurements (above) and the calculation results (below). The solid lines are the corresponding approximations.

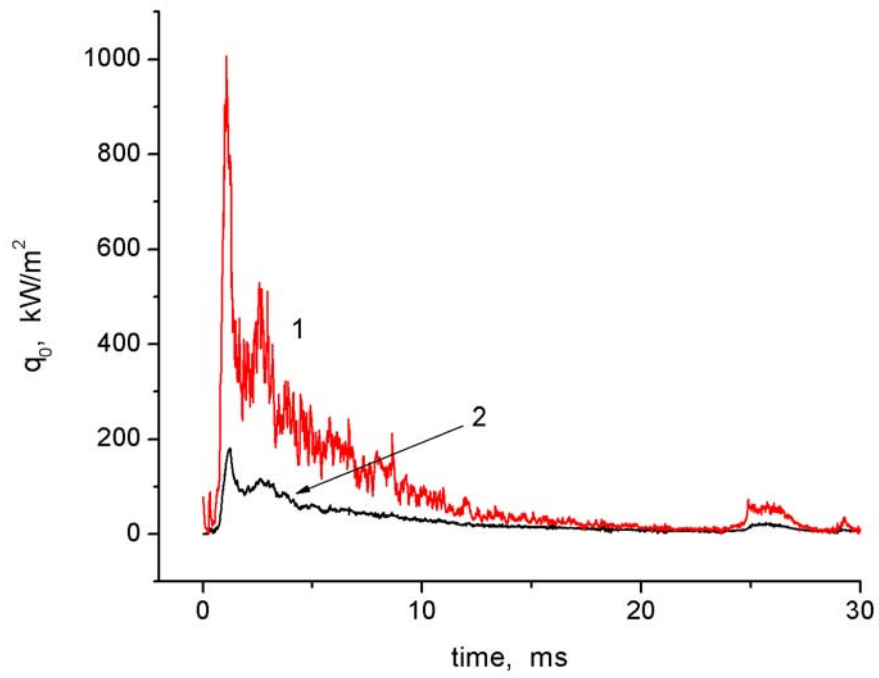


Fig.17. Variation of the heat flux recorded by the ALTP (curve 1) and GHFS (curve 2)

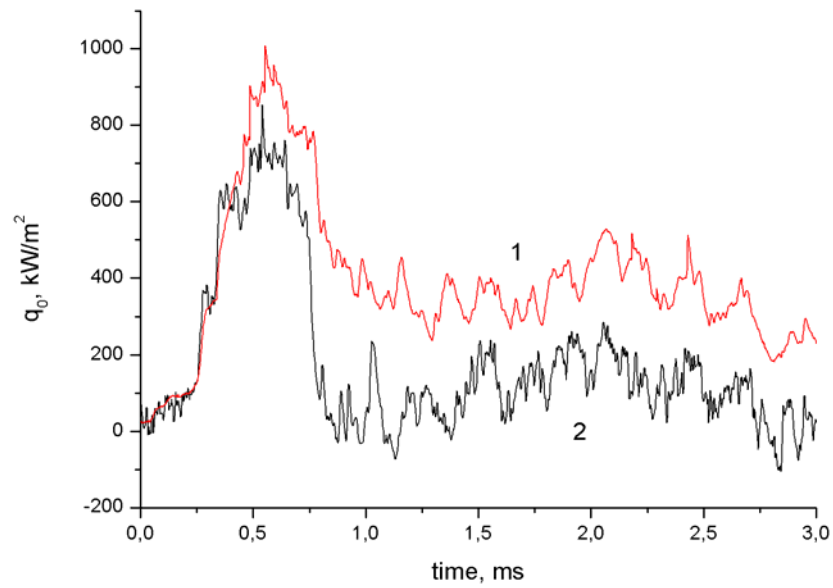


Fig. 18. Variation of the heat flux toward a plate in the supersonic flow. Curve 1 is measurements by the ALTP sensor, curve 2 is the result of processing of the GHFS signal.

NUMERICAL SIMULATION

ABSTRACT

The study of MHD control of flow structure and the wall heat flux in supersonic flows about bodies in the framework of ISTC project no.3475p was based on a contemporary approach to investigations of complicated physical processes involved which is a combination of experimental and numerical modeling. Both monatomic and molecular gases (Xe and N₂) were considered as a working medium in experiments and simulations.

For numerical investigations, a set of algorithms have been developed and demonstrated applicability to a wide range of magnetohydrodynamic phenomena in. On the basis of this set two problems have been considered, MHD control of supersonic flow in a dihedral angle and MHD control of supersonic flow about a cone-cylinder model body.

COMPRESSION FLOW IN THE DIHEDRAL ANGLE

To simulate xenon plasma compression flow in the dihedral angle a model considering the plasma as a quasi-neutral electrically conducting continuum is used. Evolution of such a medium is described by equations of magnetic hydrodynamics. Arrangement of the working section is presented in Fig. 1.

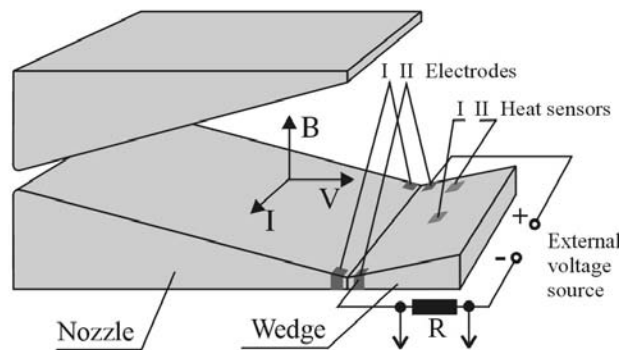


Fig.1. Working section of the Big Shock tube setup

Mathematical model

The MHD interaction has been considered within the framework of the MHD approach neglecting the induced magnetic field. Validity of this assumption follows from the below inequalities

$$l_D \ll L, \quad V_0 \ll c, \quad \tau_g = L/V_0 \gg \omega_p^{-1}, \quad \text{Re}_m \ll 1,$$

which certainly hold for the flows under study. Here, l_D is the Debye length, L is the flow length scale, V_0 is the flow velocity scale, c is the speed of light, ω_p is the plasma frequency, Re_m is the magnetic Reynolds number. The algorithm includes the Navier-Stokes equations with addition of the Joule heating and the ponderomotive force.

Under such assumptions the MHD equations can be written in the following form:

$$\frac{\partial \rho}{\partial t} + \text{div}(\rho \vec{V}) = 0,$$

$$\rho \frac{d\vec{V}}{dt} = \text{Div} \vec{P} + \vec{j} \times \vec{B},$$

$$\rho \frac{d\left(\varepsilon + \frac{V^2}{2}\right)}{dt} = \operatorname{div}(\vec{P}\vec{V}) + \operatorname{div}(\lambda_e \operatorname{grad}T) + \vec{j} \cdot \vec{E},$$

where

$$\varepsilon = c_v T = \frac{1}{\gamma-1} \frac{p}{\rho}, \quad \vec{P} = 2\mu_e \dot{S} - \left(p + \frac{2}{3}\mu_e \operatorname{div}\vec{V}\right) \vec{I} - \overline{u_i u_j}, \quad E = \frac{3}{2} p + \frac{\rho V^2}{2},$$

$$\mu_e = \mu + \mu_t, \quad \lambda_e = \lambda / \operatorname{Pr} + \lambda_t / \operatorname{Pr}_t.$$

Right parts of the momentum and energy conservation equations contain terms, describing electromagnetic effect of interaction, ponderomotive force and the Joule heat release. At that the system of equations must be completed by the Ohm's law:

$$\vec{j} = \sigma \vec{E}' = \sigma (\vec{E} + \vec{V} \times \vec{B})$$

Simple approach was used to determine intensity of electrostatic field, based on applying of the loading coefficient:

$$k = -\frac{|\vec{E}|}{|\vec{V} \times \vec{B}|} = \operatorname{const}, \quad (0 \leq k \leq 1)$$

At conditions under study it is necessary to apply a turbulence model for more precise determination of friction and heat transfer. As a first step simple one-parameter Spalart-Allmaras model was used:

$$\overline{-u_i u_j} = 2\mu_t S_{ij} / \rho, \quad \mu_t = \rho \tilde{\nu} f_{\nu 1}, \quad f_{\nu 1} = \frac{\chi^3}{\chi^3 + C_{\nu 1}^3}, \quad \chi = \frac{\tilde{\nu}}{\nu},$$

For additional variable $\tilde{\nu}$ the following equation was introduced:

$$\frac{d\tilde{\nu}}{dt} = G_{\tilde{\nu}} + \frac{1}{\sigma} \left[\nabla \cdot ((\nu + \tilde{\nu}) \nabla \tilde{\nu}) + c_{b2} (\nabla \tilde{\nu})^2 \right] - Y_{\tilde{\nu}}$$

Boundary conditions

In the inflow boundary all plasma parameters are prescribed. On the body surface the non-slip conditions are imposed. The experiments show that the temperature of the vehicle model remains constant during operation time so the heat fluxes on the body surface can be calculated at constant temperature of the surface. The model material (excepting the electrodes) is supposed to be insulator.

Numerical method

Stationary solution is obtained using time-asymptotic technique with an implicit high resolution algorithm providing the second order accuracy with respect to the spatial coordinates in the flow regions with smooth function behavior. The method is conservative shock capturing

one which is necessary in computations of supersonic flows with various non-uniformities, shock waves, etc.

Investigated domain was divided into cells. Distribution of a gasdynamic function inside a cell was assumed to be uniform; value of the function was equal to that in cell center.

Method of calculation of the convective fluxes in the set of plasma dynamic equations was based on a finite volume high resolution scheme. Considering the governing equations in vector form and performing integration over the cell volume, it is possible to obtain:

$$\frac{1}{V} \left(\frac{\partial}{\partial t} \int_V U \cdot dV + \oint_S \vec{F} \cdot \vec{n} \cdot dS \right) = R$$

here: R is the vector containing the right parts of the governing equations, V is the volume of the cell, S is the cell surface, \vec{n} is vector normal to surface S . Fluxes through cell's faces ($\vec{F} \cdot \vec{n}$) can be computed from the Riemann problem. This procedure possesses the second order accuracy over spatial coordinates, satisfies the TVD principals, and provides monotonicity of the solution.

Substituting the obtained fluxes into this equation, it is possible to write:

$$\frac{\partial U}{\partial t} = - \frac{1}{V} \oint_S \vec{F} \cdot \vec{n} \cdot dS + R$$

This equation is solved by a two-layer implicit scheme.

This method is conservative and concerns to shock-capturing methods. It provides the second order approximation over temporal coordinate as well, which is necessary to solve unsteady problems.

Block-structured computational mesh was used providing refinement in domains of stiff gasdynamic function gradients. An example of the mesh is presented in Fig. 2.

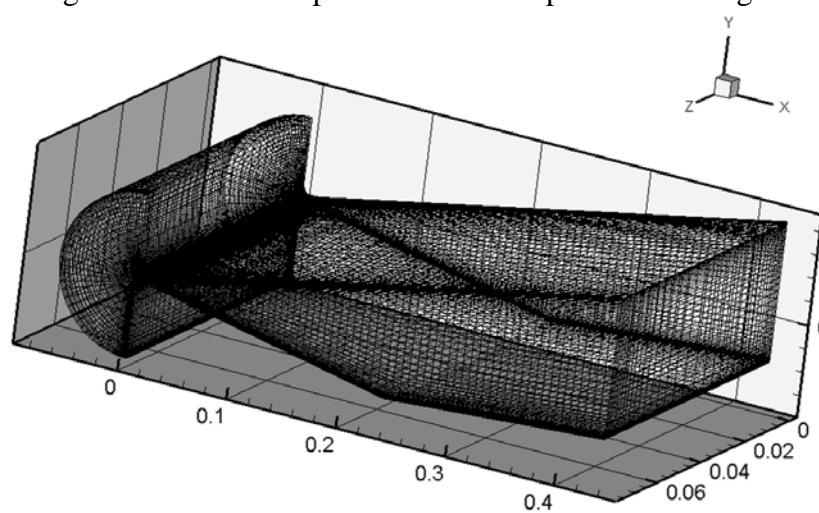


Fig. 2 Computational domain and mesh.

Some results

Figs. 3 - 9 present some results of numerical investigations of compression flow in the dihedral angle. Effect of the MHD interaction is noticeable. In the vicinity of the centerline of the dihedral angle the flow is decelerated or accelerated (depending on direction of the magnetic induction), which results in splitting of the shock wave side image (see Fig. 3 for experimental results and Figs.4 (a, b, c, d) for simulations).

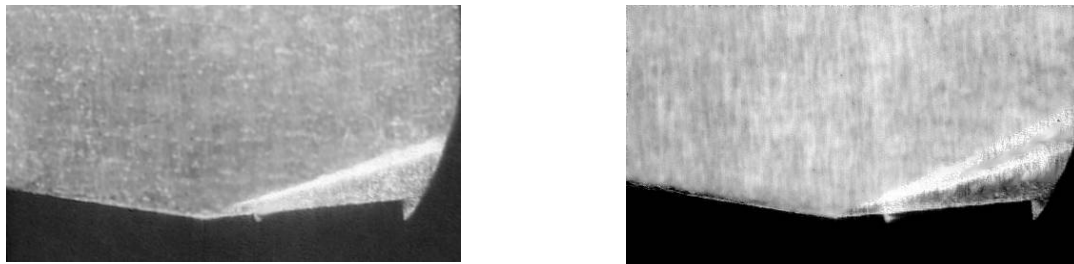


Fig.3. Schlieren photographs of the dihedral angle compression flow structures without, (a), and with, (b), the MHD interaction. Working section of the Big Shock tube setup.

$St_0 = 0.2$, $M_0 = 5.0$, decelerating ponderomotive force

DENSITY:

lateral plane - shock wave slope angle is 24° to the incoming flow direction;

middle plane - shock wave slope angle is 32° to the incoming flow direction;

dashed lines - slopes of the shock wave in the above planes.



cross-section $x=0.26$ m

(a)



(b)

$St_0 = 0.2$, $M_0 = 5.0$, accelerating ponderomotive force

DENSITY:

lateral plane - shock wave slope angle is 24° to the incoming flow direction;

middle plane - shock wave slope angle is 19° to the incoming flow direction;

dashed lines - slopes of the shock wave in the above planes.



cross-section $x=0.26$ m

(c)



(d)

Fig. 4 (a, b, c, d) Deformation of the shock wave due to MD interaction. Traces of the shock wave on the middle and lateral vertical planes

(white and red dashed lines, correspondingly).
 Decelerating, (a, b), and accelerating, (c, d), ponderomotive force

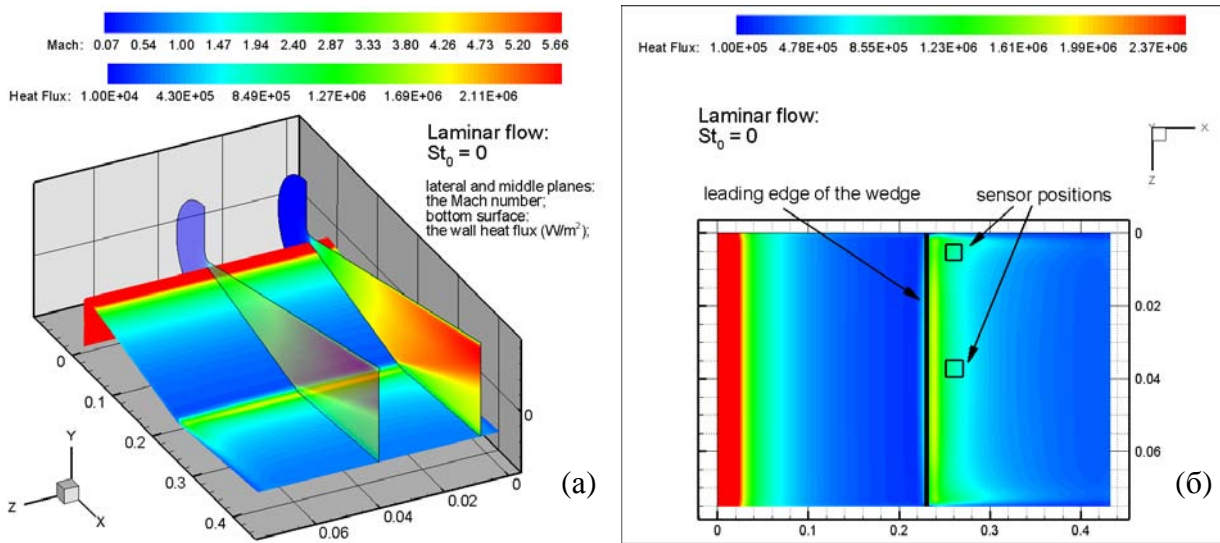


Fig. 5. Mach number and wall heat flux distributions in case of absence of MHD impact on xenon plasma laminar flow.

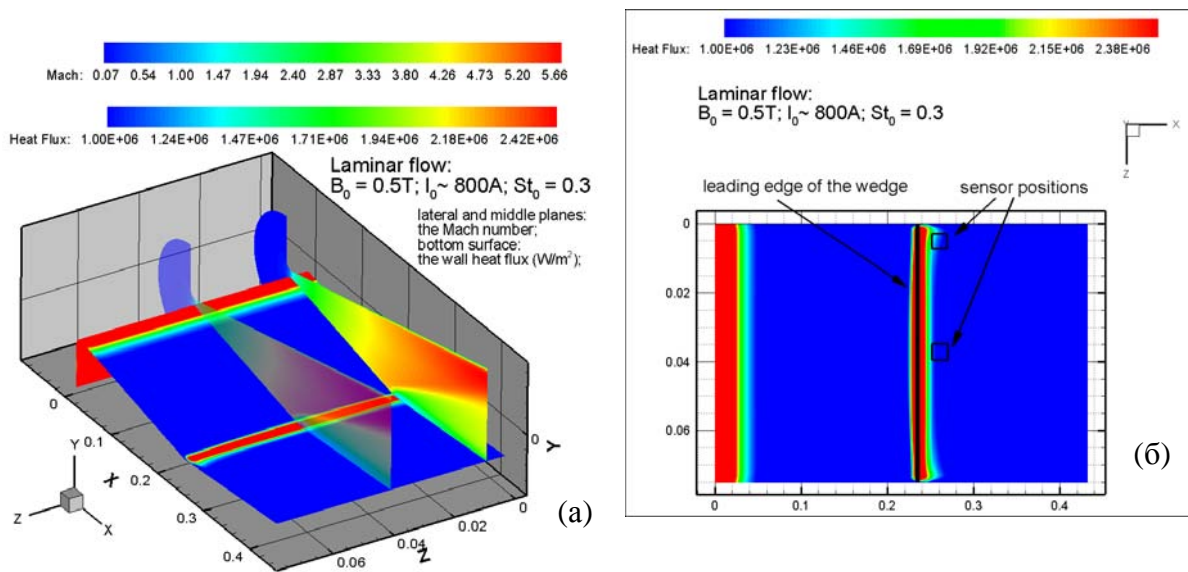


Fig. 6. Mach number and wall heat flux distributions in case of MHD impact on xenon plasma laminar flow under MHD impact.

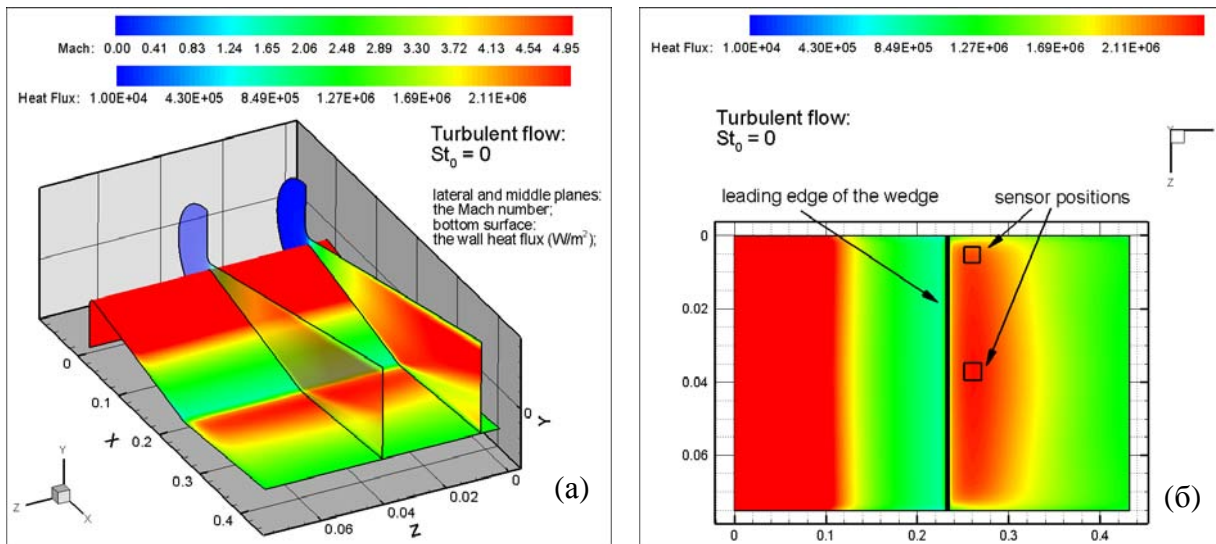


Fig. 7. Mach number and wall heat flux distributions in case of absence of MHD impact on xenon plasma turbulent flow.

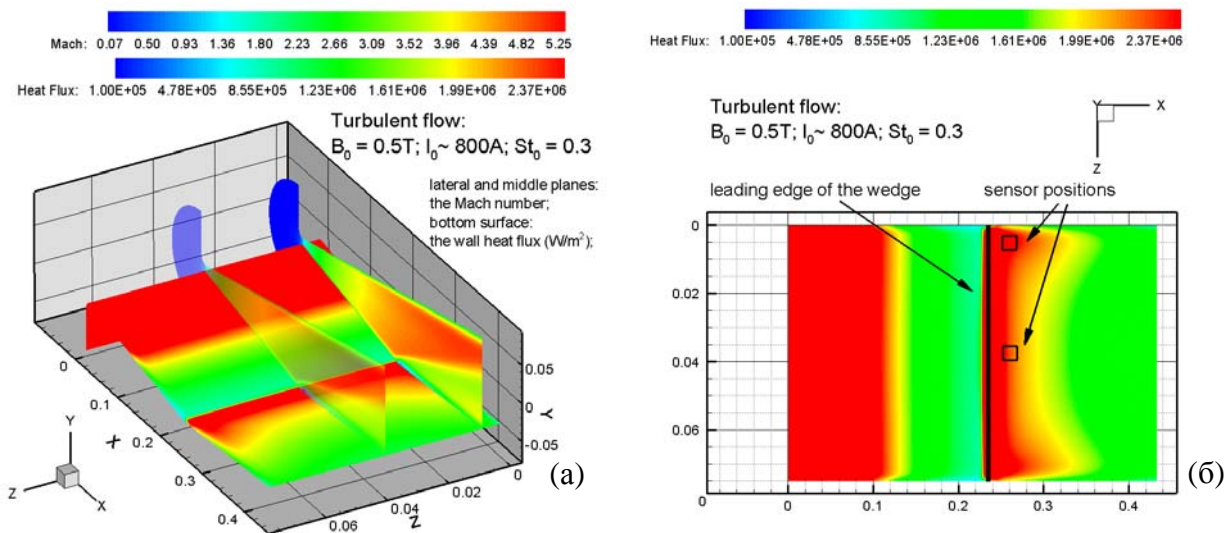


Fig. 8. Mach number and wall heat flux distributions in case of MHD impact on xenon plasma turbulent flow under MHD impact.

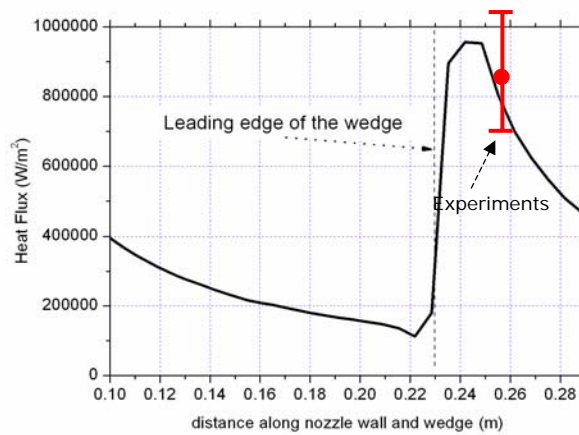


Fig.9. Wall heat flux profile along lower nozzle wall the centerline of the dihedral angle.

Combination of the experimental and numerical investigations provides profound insight into complicated processes accompanying the MHD impact on supersonic plasma flows.

Conclusions

1. Experimental and numerical investigations of the shock wave structure of the flow along a deflecting plate at an MHD impact showed that under the action of the ponderomotive force the periphery sections of the shock wave surface are curved. A numerical calculation showed that change in sign of the vector of the magnetic induction leads to change in sign of the curvature of the shock wave in its transversal cross section.

2. Investigations of the heat flux toward the plate surface in the supersonic plasma flow interacting with the magnetic field showed that the MHD effects appreciably changed the heat flux toward the body surface located in the flow. Under the experiment conditions the heat-transfer load on the surface is formed under the action of two processes: the Joule heat release providing maintenance of high plasma conductance, and heat release conditioned by the MHD influence on the supersonic flow. The MHD influence on the heat flux mainly manifests itself in the periphery flow regions, and practically does not affect the central flow region.

SUPERSONIC FLOW AROUND CONE-CYLINDER MODEL BODY

Numerical investigations have been carried out of supersonic MHD flow of weakly ionized nitrogen plasma around a cone-cylinder body at conditions corresponding to experiments on the Big Shock Tube of the Ioffe Institute of RAS.

The purpose of the carried out investigations was further validation of the formulated mathematical model and algorithm as well as revealing and the analysis of major factors determining the MHD impact on the flow. The effect of the magnetic field induced by the coil built-in the body on the plasma flow was investigated and the efficiency of the MHD interaction was estimated. At that the special attention was paid to determination of the heat and dynamic loadings on the body under study and comparison of results of flow simulation with experimental data, in particular, with wall heat flux measurements with the gradient heat flux sensors.

To enhance the efficiency of the MHD interaction a surface electric discharge was arranged between an electrode installed on the model nose and a ring coaxial electrode installed in the vicinity of the cone-cylinder conjugation (see Fig. 1). In the magnetic field induced by the coil the discharge rotates producing a domain of high plasma electric conductivity near the cone surface. This provides rise of the efficiency of the MHD interaction which is localized near the cone surface with maximum at the cone-cylinder conjugation.

The investigation showed that at the conditions under study the predominant factors of MHD impact on weakly ionized plasma flow around the body determining the flow structure are both the ponderomotive force and the Joule heating. It is worth to be mentioned that in a wide range of incoming plasma flow parameters the flow around the body is turbulent one which also significantly influence on the flow structure.

Results of numerical simulation of laminar and turbulent weakly ionized plasma flows around the cone-cylinder body under MHD interaction are presented.

Configuration and arrangement of the cone-cylinder model body are presented in Fig. 10.

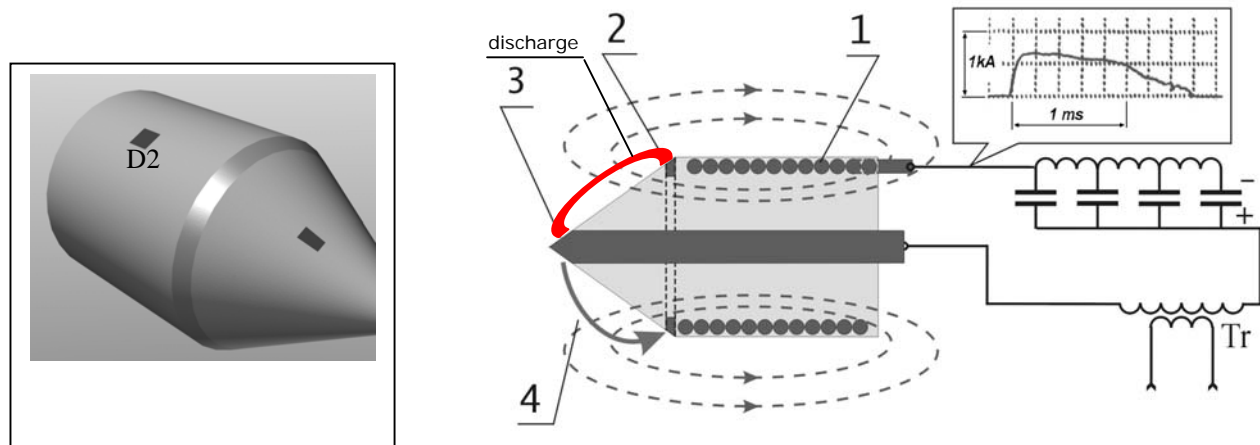


Fig. 10. Configuration and schematic diagram of the cone-cylinder body with the induction coil inside, (1), the electrodes, (2, 3), and the heat flux sensors, D1, D2.

Mathematical model

To simulate nitrogen plasma supersonic flow around the cone-cylinder model the model formulated for the compression flow in the dihedral angle was used. The model considers the plasma as a quasi-neutral electrically conducting continuum.

Numerical method

Stationary solution is obtained using time-asymptotic technique with an implicit high resolution algorithm providing the second order accuracy with respect to the spatial coordinates in the flow regions with smooth function behavior. The method is conservative shock capturing one which is necessary in computations of supersonic flows with various non-uniformities, shock waves, etc.

Structured computational mesh is used providing mesh refinement in domains of steep gradients of gas dynamic functions. Example of such a mesh is shown in Fig. 11.

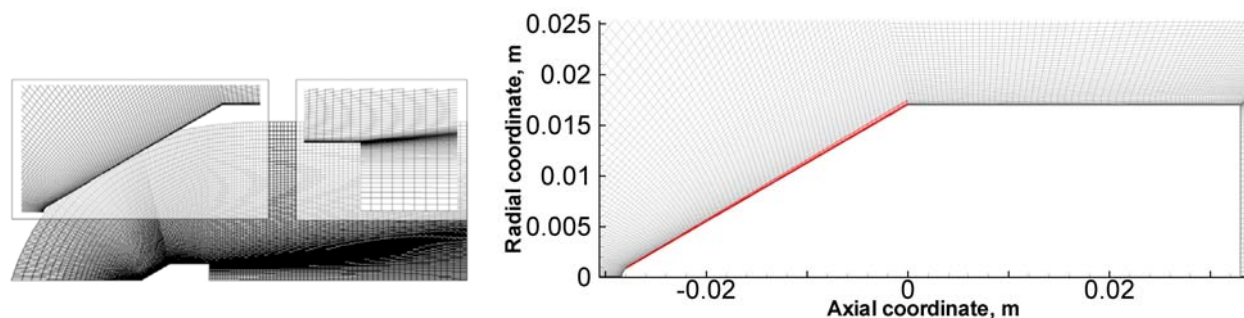


Fig. 11. An example of the block-structured computational grid.
Discharge area is marked by red.

Some results

Computations were carried out for the model body presented in Fig. 10. The magnetic coil parameters and the electric current pulse were chosen to provide the magnetic induction in coil center to be equal approximately to 1.0 T, and characteristic time of magnetic field existence was much greater than flow establishing time.

In Figs. 12 – 16 some results are presented of numerical simulation of supersonic weakly ionized nitrogen flow around the cone-cylinder body (diameter of the cylinder is 34 mm, its length is 33 mm, cone half-angle is 30° , the flow parameters correspond to those of the flow produced by the BST setup of the Ioffe Institute of RAS.

Fig. 12 demonstrates distributions of the magnetic field induction and axial component of the ponderomotive force which induced by the electric current pulse in the coil (the characteristic current pulse time is about 1.5 ms, the total current is 10^3 A). It is seen that at chosen arrangement of the induction coil domain of maximum MHD interaction is localized in the vicinity of the cone-cylinder conjugation where the induction of the magnetic field reaches 30 T.

The electric discharge between the electrode on the cone tip and on the cone-cylinder conjugation arranged to enhance the MHD interaction efficiency and produced by the electric current pulse through the induction coil rotates in the induced magnetic field with frequency about 30 kHz, that allows, comparing the rotation period and the characteristic time of plasma recombination, consider, at the present stage of the investigations, the flow as axisymmetrical.

Estimates showed that in this case the plasma electric conductivity near the cone surface is about $\sigma \approx 10^4$ S/m. This value was used in the simulations.

It is worth to be mentioned that in spite of significantly non-uniform distribution of the magnetic field induction domain of the efficient MHD interaction is localized at all surface of cone due to high density of the electric current in the discharge.

Mach number distributions are presented in Figs. 13 (a, b). Effects of the turbulence manifest itself mainly in increasing of the dynamic and heat loadings on the body. Under considered conditions MHD interaction results in noticeable decrease of the Mach number near the body, which is mainly due to temperature increase because of the Joule heating and flow deceleration because of ponderomotive force effect. Expansion of the temperature layer leads to increase of the head shock distance (increase of the head shock inclination), as well as to expansions of the boundary layer on the cylinder.

In Figs. 14 (a, b) temperature distributions near the body are shown. Intensive heating on the cone surface results in significant growth of high temperature domain and in flow deceleration.

Figs. 15 (a, b) present pressure distributions for the same regimes. It is seen that the MHD interaction leads to increase of the pressure behind the shock wave. Appreciable head shock deformation in the vicinity of maximum MHD interaction domain (cone-cylinder conjugation) is visible.

Fig. 16 demonstrates comparison of simulated wall heat flux profile along the body generatrix with experimental data. Both laminar (near the cone) and turbulent (near the cylinder) flows were simulated. Rather good agreement of the predictions and the measurements can be observed. This testifies for adequacy of the implemented mathematical model and for laminar/turbulent transition in the flow around the of test body at conditions provided by the BST setup of the Ioffe Institute.

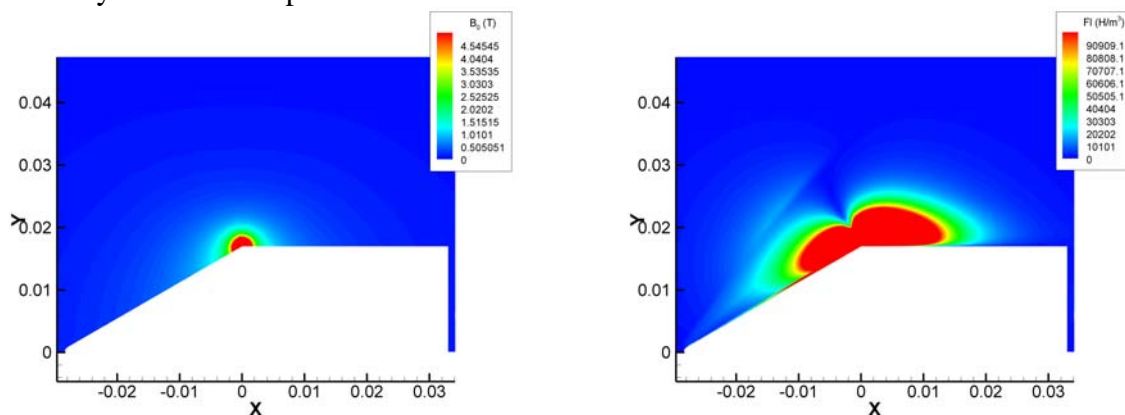


Fig. 12. Distribution of the induction of the magnetic field generated by pulse of the electric current in the induction coil (left) and distribution of axial component of the ponderomotive force (right).

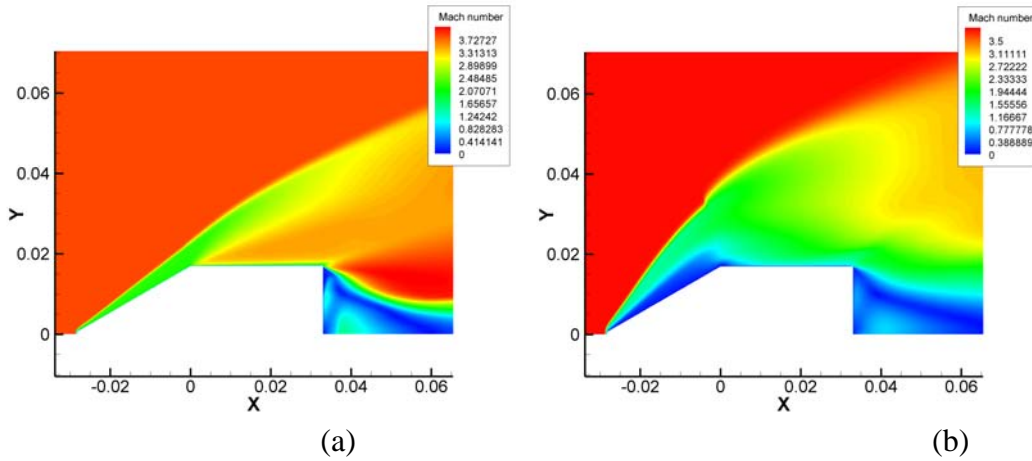


Fig. 13 (a, b). Mach number distributions; turbulent regime; (a) corresponds absence of the MHD interaction, (b) corresponds to presence of MHD interaction.

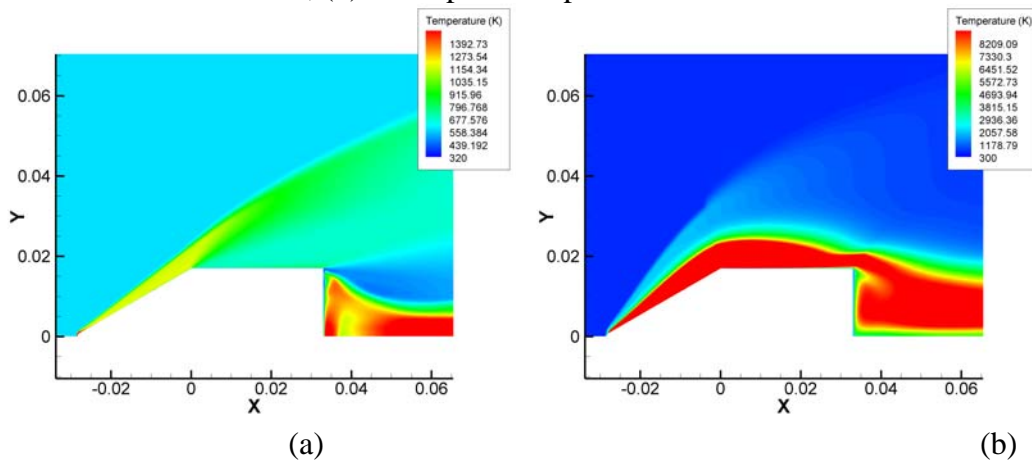


Fig. 14 (a, b). Temperature distributions ; turbulent regime; (a) corresponds absence of the MHD interaction, (b) corresponds to presence of MHD interaction.

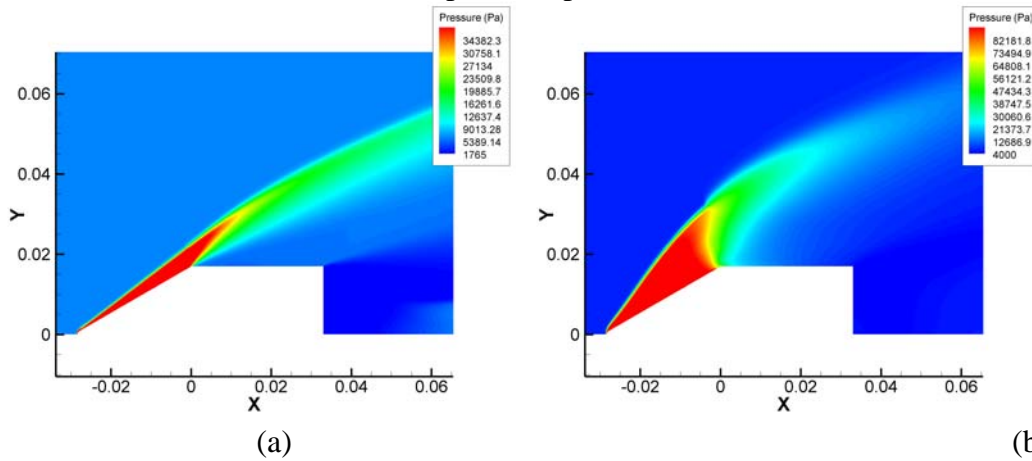


Fig. 15 (a, b). Pressure distributions ; turbulent regime; (a) corresponds absence of the MHD interaction, (b) corresponds to presence of MHD interaction.

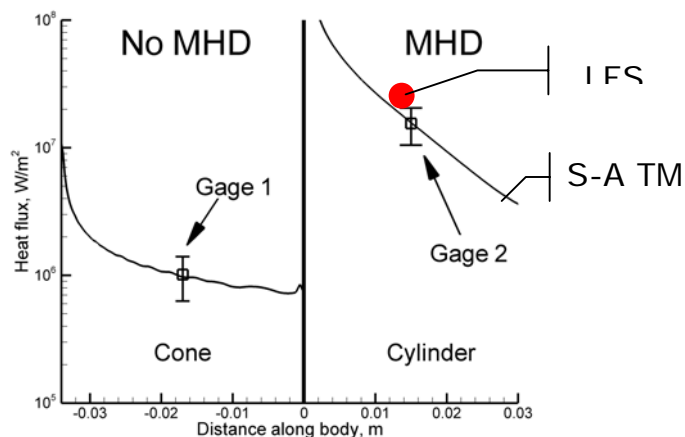


Fig. 16. Comparison of the simulated wall heat flux with the experimental data; the cone surface (without MHD interaction) and the cylinder surface (with MHD interaction).

The Task for the reported was to consider self-consistent problem of heat transfer in supersonic flow around the model body. Detailed consideration has demonstrated that during shock tube experiment heating-up of the model body (temperature rise is a few degrees Kelvin) is of significantly less importance for wall heat flux measurements than heat transfer inside the sensor.

That is why the main attention in this period was paid to investigation of effects of turbulence models. A Large Eddy Simulation Turbulence Model (LES TM) seems to be perspective for problems characterized by external influence, such as MHD impact. Since transport of mass, momentum, and energy of turbulent medium is mainly due to the large eddies this process can be simulated directly on the basis of “filtered” Navier-Stokes equations supplied with specific MHD terms, the Joule heating and the ponderomotive force. Small eddies are less dependent on the external influence and can be described by a subgrid model. Besides all such an approach probably enables one to use more coarse numerical grids and large time-steps in comparison with other turbulent models. In this investigation LES TM was used with the Smagorinsky model for subgrid scale.

Some results of simulation of the supersonic nitrogen plasma flow around the model body with the LES TM are presented below.

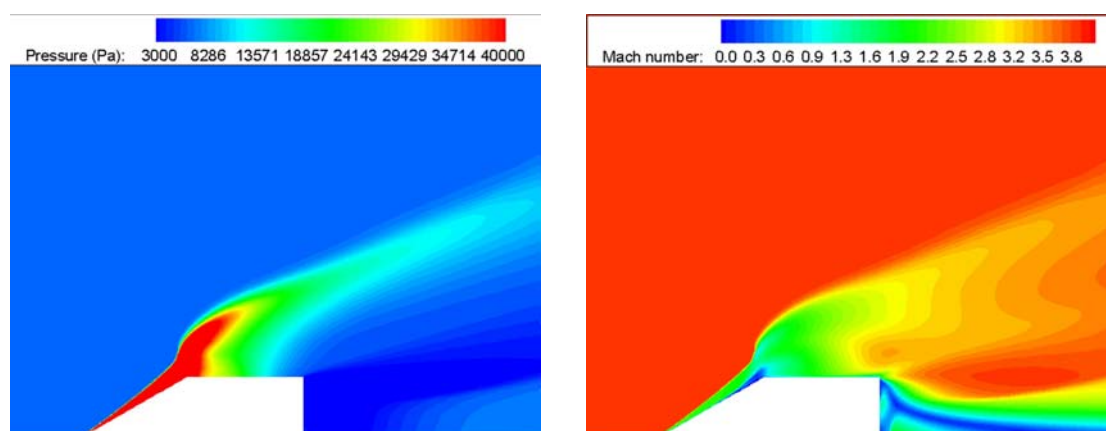


Fig. 17. Mach number, (a) and pressure, (b), distributions; turbulent regime, MHD impact on the flow

Effect of the turbulence model manifests itself in such an important process as the Joule heating. This results in variation of the flow structure. Significant deformation of the shock wave in the vicinity of cone-cylinder conjunction is seen in Figs. 17, 18, and in a rise of the wall heat flux (see Fig. 16)

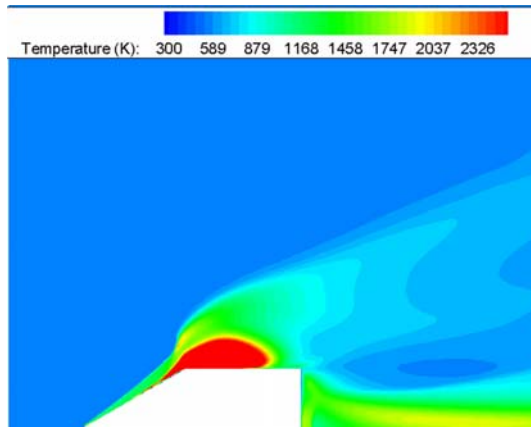


Fig. 18. Temperature distribution; turbulent regime, MHD impact on the flow

Conclusion

Thus, in course of the simulations under the Project program with the help of the formulated mathematical model and the numerical method computations were carried out of laminar and turbulent supersonic weakly ionized nitrogen flows around cone-cylinder body under the MHD impact. The algorithm was modified which results in increase of order of approximation in temporal coordinate till second. The proposed algorithm provides an opportunity to simulate structure of the supersonic flow around the body and to determine the dynamic and heat loadings on the body.

On the basis of the presented results obtained in the framework of this rather rough model it is possible to conclude that under considered parameters of the magnetic field and the electric discharge the localized MHD interaction results in noticeable rearranging of flow structure.

It is shown that the proposed way of the MHD flow control results in increase of the wall heat flux.

As regards to aerodynamic drag of such a body with MHD interaction it can be note that rearrangement of the base flow accompanying the MHD impact decreases essentially effect of drop of the drag on the cone and cylinder.

Effect of turbulence models was considered for the Spalart-Allmaras turbulence model (S-A TM) and the LES TM. Noticeable change of the flow structure and rise of the wall heat flux were demonstrated.

The predictions of the simulation are in good agreement with experimental data obtained on the BST setup of the Ioffe Institute of RAS.

Attachment 1: List of published papers and reports with abstracts

1. Sakharov V.A., Mende N.P., Bobashev S.V., Sapozhnikov S.Z., Mityakov V.Yu., Mityakov A.V. Thermal measurements at the body surface in a supersonic nitrogen flow. 2006, Tech. Phys. Lett., v.32, 7, pp: 621-623.

Abstract—Measurements of the heat flux toward the surface of a body of revolution in a supersonic nitrogen flow with Mach number 4 were carried out. Inside the body, an electromagnetic facility is mounted which generates a gas-discharge plasma between electrodes flush-mounted at the body surface. The plasma rotates around the body surface and significantly influences the supersonic flow. During operation of the electromagnetic facility, the heat flux toward the body surface increases and depends on the direction of the electric current flowing through the plasma. The heat flux was measured by fast-response gradient heat flux sensors based on anisotropic bismuth crystal.

2. Sakharov V.A., Mende N.P., Bobashev S.V., Van Wie D.M. Magnetohydrodynamic control of a supersonic flow about a body. 2006, Tech. Phys. Lett., v.32, 7, pp: 618-620.

Abstract—The structure and principle of operation of an electromagnetic facility capable of controlling a supersonic flow about a body of revolution are described, by means of which gas-discharge plasma formed between electrodes flush-mounted on the body is driven over its surface by a magnetic field. It is shown that the frequency of rotation of the gas-discharge plasma strongly depends on the direction of electric current flowing through the facility, as well as on the pressure of ambient gas. Experimental results demonstrating the effective magnetohydrodynamic control over the structure of supersonic nitrogen flow about the body of revolution at a Mach number of 4 are presented.

3. Reznikov B.I., Mende N.P., Popov P.A. Sakharov V.A., Shteinberg A.S. Determining heat flux from surface temperature measurements in pulsed gasdynamic processes. 2008, Tech. Phys. Lett., v.34, 8, pp.: 656-658.

Abstract—The surface temperature of a body of revolution in a pulsed supersonic nitrogen flow has been measured using anisotropic thermoelements based on bismuth single crystals. A method for calculating the heat flux toward the body surface using data on the surface temperature variations is proposed, which is based on solving the heat conduction equation in a semibounded space. The errors of temperature measurements and heat flux calculations are estimated using linear regression analysis.

4. Technical report no. 1. ISTC Project 3475p. July 2006.

Abstract—In accordance with the 1st quarter work plan (May – July 2006) of Project no. 3475, a flat plate has been designed, fabricated and mounted in the test section of the double-diaphragm shock tube at the Ioffe Institute. Two pair electrodes are embedded into the nozzle and plate walls flush with their surfaces. The electrodes serve for passing an electric current through the supersonic flow of a weakly ionized gas. As a material for the electrodes we choose brass possessing a high conductance and acceptable heat stability.

Heat sensors on the base of anisotropic bismuth crystal have been tested by producing heat load with the use of radiation of a laser operating in various regimes. Evaluation of the response time of the sensors to a pulsed heat load with the known time parameters has been conducted. The response time of the sensors completely corresponds to the requirements of the forthcoming experiments.

Algorithms and applied codes for numerical simulation of an essentially nonsteady-state hypersonic flow of a viscous heat-conducting plasma exposed to a pulsed magnetic field were adjusted to the problem to be solved.

5. Technical report no. 2. ISTC Project 3475p. October 2006.

Abstract---The report contains results of investigations conducted during the second stage according to ISTC Project No. 3475p "Control of heat fluxes on the surface of the body streamlined by supersonic flow with the help of MHD method".

The subject of the investigations is the possibility of experimental modeling of an impact on a supersonic flow by magnetic field established by an inductor housed inside a body of revolution by means of inducing a closed ring electric current flowing around the body in the plasma. Experimental investigations were carried out in parallel with numerical simulation of the process.

In accordance with the total set of the Project, an analysis of operation of heat sensors is carried out aimed at evaluation of their characteristics and possibility of their application in investigations of pulsed processes in the presence of a strong electromagnetic interference.

6. Technical report no. 3. ISTC Project 3475p. January 2007.

Abstract---Analysis of the influence of a magnetic field on the heat flux toward a plate will be preceded by description of a new approach to treatment of the measurement results acquired with the help of the gradient heat flux sensor (GHFS) based on Bismuth monocrystal [1]. The necessity of that arose because of disagreement between the sensor signals and the existing notions about behavior of the heat flux caused by pulsed heat-transfer loads. In particular, it is referred to measurements of the heat flux caused by normal reflection of a shock wave from a rigid wall and heat flux toward the surface of a cone in a supersonic flow, as well as to the sensor response to a laser pulse of a small duration.

7. Technical report no. 4. ISTC Project 3475p. April 2007.

Abstract---In the interim report of the second stage of the present project a detailed description of the experimental and numerical investigations aimed at studying interaction between a supersonic flow of a weakly ionized xenon plasma flow about an axisymmetric body and a magnetic field was given. In the same report, results of experiments demonstrating an impact of a pulsed magnetic field on an immovable xenon plasma were presented.

The objective of the present report consists in analyzing the results mentioned above and in estimating possibility of experimental modeling of magnetohydrodynamic (MHD) influence on a supersonic flow with no means of additional ionization of the gas flow.

8. Technical report no. 5. ISTC Project 3475p. July 2007.

Abstract---The report contains results of tests of an axisymmetric object designed in such a way that all components needed for local magnetohydrodynamic impact on the flow of a molecular gas about the object are located inside it or at its surface.

The second part of the report is devoted to analysis of gradient heat flux sensors in the presence of strong electromagnetic fields affecting the flow, evaluation of the acceptable dimensions of the sensors and choice of their location at the test object. Estimation of the accuracy of determination of the heat flux on the base of measurements of the model surface temperature is carried out.

9. Technical report no. 6. ISTC Project 3475p. October 2007.

Abstract---Comparison between responses of the Gradient Heat Flux Sensor (GHFS) on the base of anisotropic Bismuth crystal and Atomic Layer Thermopile (ALTP) to an impact produced by a supersonic flow behind a shock wave is carried out. Analysis of the sensor signals showed that for processes with the characteristic time exceeding 10 ms the GHFS may be used for direct measurements of the heat flux toward a surface under study.

A technique is proposed for processing of the GHFS signal that makes it possible to determine the heat flux in processes with characteristic time ~ 1 ms. It is shown that this technique allows one to study heat flux pulsations with a frequency of ~ 20 kHz.

The carried out tests of the GHFS showed again that it possesses a high speed of response (~ 30 ns), high sensitivity (~ 1 mV/K), and is a unique tool for conducting measurements in pulsed processes with a duration of ~ 1 ms accompanied by strong electromagnetic noises. In this respect the GHFS has no analogs.

10. Technical report no. 7. ISTC Project 3475p. January 2008.

Abstract---In the reported period numerical investigations have been carried out of supersonic MHD flow of weakly ionized nitrogen plasma around a cone-cylinder body at conditions corresponding to experiments on the Big Shock Tube of the Ioffe Institute of RAS. Among tasks of this stage of the Project there was a selection of the flow regime and plasma parameters in the vicinity of the body. However/ this part of the work has been done at the previous stages of the investigations of the flows about the body (see Report no. 2) flows in dihedral angle (see Report no. 3)

11. Annual technical report. ISTC Project 3475p. April 2008.

Abstract---The report is a short summary of the results of investigations conducted during the period May 2007 –April 2008 according to ISTC Project No. 3475p “Control of heat fluxes on the surface of the body streamlined by supersonic flow with the help of MHD method”. Detail information can be found in Technical Reports #5 (July 2007), #6 (October 2007) and #7 (January 2008). Technical Report no. 8 is a part of this Report and contains the results mainly in accordance with Task no. 8 of the Project.

12. Technical report no. 9. ISTC Project 3475p. July 2008.

Abstract---Conditions of measurements of the heat flux in the presence of a gas discharge near a body under study and a magnetic field induced by an inductor housed inside the body are considered. A safe location of the heat flux sensor on the body surface is chosen with making allowance for the possibility to record the heat influence of the gas discharge. The experiments carried out confirmed correctness of the decision accepted.

The specific features of the heat sensor fabricated on the base of anisotropic Bismuth monocrystal demanded consideration of the mechanism of the processes proceeding in the sensor, including making allowance for the influence of a substrate at which the sensor is installed. It is shown that at characteristic durations of the processes under study, processing of the signal of the “thick” Bismuth sensor enables one to obtain data about the heat flux comparable with measurements by a thin-film sensors whose signal is calibrated directly in terms of the heat flux. A conclusion is drawn that when making allowance for high noise immunity and short response time of the Bismuth sensor it must be recognized as the most applicable in the presence of strong electric and magnetic fields.

13. Final technical report. ISTC Project 3475p. October 2008.

Abstract---The first section of the final report on the works according to ISTC Project (2006–2008 including the extension of the Project for 9th and 10th stages) contains the review of the basic experimental results of MHD influence on a supersonic gas flow, results of numerical simulation of the processes in a supersonic viscous flow as well as the analysis of them. The second section of the report is devoted to development of a technique for employment of the gradient heat flux sensor (GHFS) which at present is the only accessible instrument being capable of functioning in the presence of strong electromagnetic interference.

The investigation is carried out of the MHD influence on the flow about two models in the shape of a cone mated with a cylinder. At the cone vertex and along the mating line two

electrodes are located between that an electric discharge is implemented, and inside the cylindrical parts magnetic inductors are housed. One of the models is equipped with a magnetic core inside the inductor. An appreciable difference between the influences on the gas flow about these two models was detected.

Dependence of the MHD influence on the flow about the models depending on the polarity of connection of the electrodes to an external voltage source is found.

Because of the large thickness of the GHFS its signal is proportional to the temperature but not to the heat flux, a procedure of transformation of the GHFS signal into the heat flux is developed. Evaluations of the errors of the temperature measurements and determination of the heat flux is carried out.

The comparison is drawn between the results obtained with the help of the GHFS and the data of direct measurements by the Atomic Layer Thermo Pile. The conclusion is drawn on the applicability of the GHFS and technique of processing of its signal in investigations of pulsed magnetohydrodynamic processes of a moderate duration (~ 1 ms).

Attachment 2: List of presentations at conferences and meetings with abstracts

1. Sakharov V.A., Mende N.P., Bobashev S.V. An Electromagnetic Facility for Producing an Impact on a Supersonic Flow about a Body of Revolution. The 6th Sino-Russian High-Speed Flow Conference. 2006.

Abstract---An approach to implementation of a magnetohydrodynamic (MHD) impact on a supersonic nitrogen flow is discussed. For MHD interaction the working gas must be ionized. A shock-heated nitrogen plasma quickly recombines when expanding through a supersonic nozzle. For this reason, in the laboratory experiment it is necessary to apply means providing an additional ionization of the gas in the test section in front of a body under study. An electromagnetic facility for this purpose was designed, manufactured, and tested. The experiments were carried out at the Ioffe Institute double-diaphragm shock tube. The results of the tests are presented.

2. Bobashev S., Erofeev A., Lapushkina T., Mende N., Poniaev S., Sakharov V., Vasilieva R., Van Wie D.M. Recent results on MHD flow control at Ioffe Institute. Int. Space Planes Hypersonics Syst. Technol. Conf., v.2, c: 987-1001. 2006. AIAA.

Abstract---This paper is a review of the investigations carried out at the Ioffe Physico-Technical Institute in collaboration with the Johns Hopkins University under the support of the EOARD during 2001 – 2006 years. These investigations were devoted to searching for ways and means of affecting a supersonic flow of a weakly ionized gas by an electromagnetic impact aimed at the magnetohydrodynamic (MHD) control of gas flows. In the course of the experimental investigations the authors were studying magnetohydrodynamic processes in supersonic xenon and nitrogen flows over plane models affected by external electric and magnetic fields, and, at the latest stage, about a body of revolution containing all components of the electromagnetic system inside itself. The results obtained evidence possibilities of an effective control of the shock wave structure of supersonic gas flows by MHD method. Also first attempts to measure heat flux toward the body surface under the interaction were made. Some initial results of measurements of the heat flux are presented.

3. Bobashev S.V., Golovachov Yu.P. Chernyshev A.S., Mende N.P., Sakharov V.A., Schmidt A.A., Van Wie D.M. Experimental and numerical investigations of localized MHD interaction in supersonic nitrogen flow about conical body. Coll. Tech. Pap. AIAA Plasmadynam. Lasers Conf., v.1, pp.: 168-174. 2007.

Abstract---This paper presents some results of numerical simulation of supersonic N₂ flow about “cone-cylinder” body. The incoming flow parameters correspond to those provided by the Big Shock Tube setup of the Ioffe Institute (Mach number $M=3.9$, $T_0=575$ K, $p_0=6383$ Pa). The plane of the induction coil coincides with that of cone-cylinder conjugation. The coil radius is equal to that of the cylinder. Parameters of the coil, electrodes, and the electric current pulse were chosen to provide the magnetic induction, B , equal to 1 T in the coil center and the total electric current of the discharge, I , equal, approximately, to 103 A. The characteristic times of the existence of the magnetic field and the electric current are longer than the time of flow development. Thus the flow and the MHD interaction can be considered as stationary.

4. Bobashev S.V., Mende N.P., Sakharov V.A., Van Wie D.M. Magnetohydrodynamic influence on a supersonic nitrogen flow about a body of revolution. Collect. Tech. Pap. Aeros. Sci. Meet., v.24, pp.: 17007-17010. 2007.

Abstract---An approach to implementation of a magnetohydrodynamic (MHD) impact on a supersonic nitrogen flow is discussed. For MHD interaction the working gas must be ionized. A shock-heated nitrogen plasma quickly recombines when expanding through a supersonic

nozzle. For this reason, in the laboratory experiment it is necessary to apply means providing an additional ionization of the gas in the test section in front of a body under study. An electromagnetic facility for this purpose was designed, manufactured, and tested. The experiments were carried out at the Ioffe Institute double-diaphragm shock tube. The results of the tests are presented.

5. Bobashev S.V., Mende N.P., Sakharov V.A., Sapozhnikov S.Z., Mityakov V.Yu., Mityakov A.V. Thermal measurements at the body surface in a supersonic nitrogen flow

Collect. Tech. Pap. Aeros. Sci. Meet., v.4, pp.: 2605-2608. 2007

Abstract---Measurements of the heat flux toward the surface of a body of revolution in a supersonic nitrogen flow with Mach number 4 were carried out. Inside the body, an electromagnetic facility is mounted which generates a gas-discharge plasma between electrodes flush-mounted at the body surface. The plasma rotates around the body surface exerting appreciable influence on the supersonic flow. It is found out that during operation of the electromagnetic facility, the heat flux toward the body surface increases and depends on the direction of the electric current flowing through the plasma. The heat flux was measured by heat flux sensors with a high speed of response.

6. Bobashev S., Golovachov Yu., Chernyshev A., Kurbatov G., Mende N., Sakharov V., Schmidt A., Van_Wie D. Supersonic Flow about Wedge: MHD Impact on Flow Structure and Heat Flux. 46th AIAA Aerospace Sciences Meeting and Exhibit , Reno, Nevada, Jan. 7-10, 2008, pp.: 2008-1094.

Abstract---This paper presents some results of experimental and numerical investigations of structure of supersonic plasma flow about a wedge. Variations of the bow-shock wave shape and the heat flux to the wedge surface due to MHD impact is considered. Flow separation induced by interaction of the bow-shock wave with the boundary layer on the nozzle wall is also investigated.

7. Bobashev S.V., Mende N.P., Popov P.A., Sakharov V. A., Van Wie D. M. Magnetohydrodynamic Influence on a Supersonic Flow. 46th AIAA Aerospace Sciences Meeting and Exhibit , Reno, Nevada, Jan. 7-10, 2008.

Abstract---The first section of the final report on the works according to ISTC Project (2006–2008 including the extension of the Project for 9th and 10th stages) contains the review of the basic experimental results of MHD influence on a supersonic gas flow, results of numerical simulation of the processes in a supersonic viscous flow as well as the analysis of them. The second section of the report is devoted to development of a technique for employment of the gradient heat flux sensor (GHFS) which at present is the only accessible instrument being capable of functioning in the presence of strong electromagnetic interference.

The investigation is carried out of the MHD influence on the flow about two models in the shape of a cone mated with a cylinder. At the cone vertex and along the mating line two electrodes are located between that an electric discharge is implemented, and inside the cylindrical parts magnetic inductors are housed. One of the models is equipped with a magnetic core inside the inductor. An appreciable difference between the influences on the gas flow about these two models was detected.

Dependence of the MHD influence on the flow about the models depending on the polarity of connection of the electrodes to an external voltage source is found.

Because of the large thickness of the GHFS its signal is proportional to the temperature but not to the heat flux, a procedure of transformation of the GHFS signal into the heat flux is developed. Evaluations of the errors of the temperature measurements and determination of the heat flux is carried out.

The comparison is drawn between the results obtained with the help of the GHFS and the data of direct measurements by the Atomic Layer Thermo Pile. The conclusion is drawn on the applicability of the GHFS and technique of processing of its signal in investigations of pulsed magnetohydrodynamic processes of a moderate duration (~ 1 ms).